

Oxygen Isotopes in Mantle and Crustal Magmas as Revealed by Single Crystal Analysis

Ilya Bindeman

*Department of Geological Sciences
University of Oregon
Eugene, Oregon, 97403-1272, U.S.A.
bindeman@uoregon.edu*

PART I: INTRODUCTION

Oxygen is the most abundant element in the Earth's crust, mantle, and fluids and therefore its isotopic composition provides robust constraints on magma genesis. Application of oxygen isotope geochemistry to volcanology and igneous petrology provides a much needed foundation for radiogenic isotope and trace element approaches. Since isotope fractionations at high temperature are small, there is a demand for high analytical precision in order to recognize and interpret small (tenths of permil) variations in isotopic composition. Recently improved analytical techniques involving lasers and ion microprobes, and reduction in sample and spot size, has painted a picture of isotope complexity on a single crystal scale that is helpful in interpreting magma genesis and evolution. In this chapter a review is provided for several classic examples of silicic and basic magmatism, including Yellowstone and Iceland, that shows isotope zoning and heterogeneity reaching several permil. Isotope heterogeneity fingerprints crystal sources and provides constraints on diffusive and recrystallizational timescales. These new lines of evidence reveal that magma genesis happens rapidly, at shallow depths, and through batch assembly processes.

Oxygen isotope geochemistry spans more than 50 years of investigation and is the most developed among other traditional (e.g., C, N, H, S, Li, B) and less-traditional (e.g., Fe, Mo, Cu) stable isotope systems. While we provide basic concepts of isotope fractionation below, the reader is referred to three prior RiMG volumes on stable isotopes (Valley, Taylor, and O'Neil 1986 – volume 16; Valley and Cole 2001 – volume 43; Johnson et al. 2004 – volume 55), and the Hoefs (2005) and Sharp (2006) textbooks for greater treatment and historic perspective. Finally this Chapter does not deal with oxygen isotopic variations in meteorites and planetary igneous materials, and interested readers are referred to RiMG volume 68, "Oxygen in the Solar System" (MacPherson et al. 2008).

The remaining novel aspects of oxygen isotope geochemistry of igneous and metamorphic rocks are related to continuing application of laser fluorination analysis to phenocrysts that provide superior analytical precision to other methods. In particular, 1) Many topical studies should include major element oxygen measured at new analytical levels as a component in multi-isotope and trace elemental investigation, 2) Older studies that relied on whole-rock methods should be reassessed, 3) Many igneous systems such as continental and oceanic flood basalts, large silicic igneous provinces, and island arc magmas should be reevaluated, 4) Oxygen isotopes should be studied on a single crystal level. This Chapter outlines the perspective that magmatic crystals should be studied individually when possible, or by size fractions, to demonstrate whether crystals are isotopically homogeneous and is in equilibrium with other minerals within common host magma. As is demonstrated below, in many classic

examples of igneous systems around the world, magmatic crystals are not in equilibrium and thus bulk phenocryst oxygen isotope analysis does not reveal the full details of petrogenesis, nor do they provide a proxy for magmatic values.

Basics of oxygen isotope variations in nature and their causes

Oxygen consists of three isotopes: ^{16}O (99.76%), ^{17}O (0.04%), and ^{18}O (0.2%). Mass-dependent, oxygen isotopic variations are described through a ratio of ^{18}O to ^{16}O and the delta notation that is traditionally used in stable isotope geochemistry:

$$\delta^{18}\text{O} = (R_{\text{SA}}/R_{\text{ST}} - 1) \times 1000 \quad (1)$$

where R_{SA} and R_{ST} are absolute ratios of $^{18}\text{O}/^{16}\text{O}$ in sample and standard and the standard is Vienna Mean Standard Ocean Water (VSMOW) with $^{18}\text{O}/^{16}\text{O}$ absolute ratios of 0.020052 (Baertschi 1976). A $\Delta^{18}\text{O}$ measure of variation between the sample and the standard is in permil (‰), or part per thousand. It is not recommended to use any other standard (e.g., PDB) when describing oxygen isotopic variations in nature since it only causes confusion. The multiplication factor of 1000 is used to display natural isotope variations in whole numbers and not fractions; it is used because isotope variations due to chemical or physical processes in nature are small, in the third or second decimal place of the $^{18}\text{O}/^{16}\text{O}$ ratio.

Oxygen isotopic variations on Earth span about 100‰ (Fig. 1). Half of these variations, and nearly all negative $\delta^{18}\text{O}$ values are occupied by meteoric waters that are isotopically-light as a result of Rayleigh distillation upon vapor transport and precipitation. Silicate rocks and magmas occupy the positive part of this diagram with the absolute majority of mantle rocks, basaltic magmas and chondritic meteorites plotting in a narrow range of 5.5 to 5.9‰. Silicate, oxide, carbonate, and phosphate minerals and igneous, sedimentary, and metamorphic rocks such as carbonates and especially diatoms that precipitate from water at low temperatures are the highest $\delta^{18}\text{O}$ materials because of large positive isotope fractionation factors between silica, carbonates and water at low temperatures (e.g., Friedman and O'Neil 1977; Chacko et al. 2001; Hoefs 2005). Metasedimentary rocks and igneous rocks such as S-type granites inherit high- $\delta^{18}\text{O}$ supracrustal signature from the source, while rocks that represent remelting of hydrothermally altered rocks that interacted with low- $\delta^{18}\text{O}$ meteoric water at high-temperature are low- $\delta^{18}\text{O}$ (see below).

Equilibrium isotope fractionation factors between minerals and melts. The equilibrium isotope fractionation factor is defined as:

$$\alpha = R_{\text{A}}/R_{\text{B}} \quad (2)$$

where R_{A} and R_{B} are absolute isotope ratios of individual, coexisting minerals at equilibrium. Since α variations are typically in the second or third decimal point, a more convenient parameter, $1000\ln\alpha$ is used.

Because of the difference in chemical bonds affecting vibrational frequencies of oxygen in minerals, a heavier isotope of oxygen partitions itself into a mineral with stronger (more covalent) Si-O-M bonds. As a general rule, isothermal high- T distribution of ^{18}O among coexisting igneous phases is explained by the proportion of Si-O and M-O bonds (Taylor 1968; Zheng et al. 1993a,b; Chiba et al. 1989; Hoefs 2005), while the cation identity in homovalent substitution (e.g., Fe vs. Mg) plays an insignificant third order role. Thus the common igneous minerals will become progressively lighter from quartz (pure silicate) to magnetite (pure M-O oxide). For example, a polymineralic granite at 850 °C with the whole-rock value of 7.8‰ will have decreasing $\delta^{18}\text{O}$ values of its constituent minerals in this sequence: quartz (8.2‰) > albite \approx K-Fsp (7.5‰) > anorthite (6.6‰) > zircon (6.4‰) \geq pyroxene (6.3‰) \approx amphibole \geq biotite \geq garnet \approx olivine (6.1‰) > sphene (5.4‰) \geq ilmenite (4.9‰) > apatite \geq magnetite (3.5‰). The quoted $\delta^{18}\text{O}$ values were calculated using experimental and empirical fractionation factors (e.g., Taylor and Sheppard 1986; Chiba et al. 1989; Zheng 1993a,b; Chacko et al. 2001; Valley

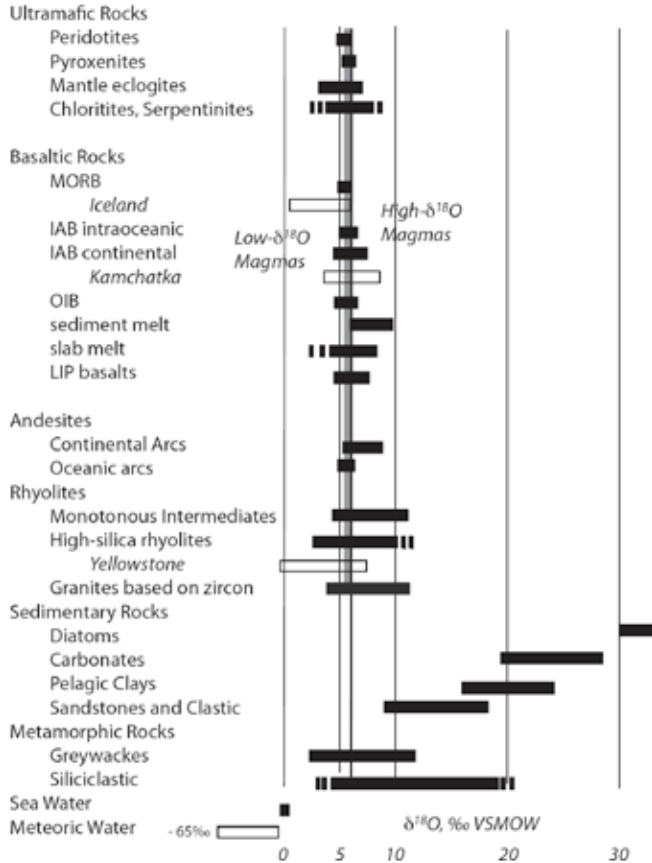


Figure 1. Oxygen isotopic variations in magmas and rocks on Earth. Gray band between 5.5 and 5.9 represents “normal- $\delta^{18}\text{O}$ magmas” for ultramafic and basaltic rocks that constitute predominant mantle and products of its melting; closed system differentiation of such magma into andesite and rhyolite that show normal $\delta^{18}\text{O}$ values of 5.8 to 6.5 permil (Fig. 4). High- $\delta^{18}\text{O}$ rocks and magmas result from low-temperature precipitation or interaction with sea water involving large positive $1000\ln\alpha_{\text{mineral-water}}$ isotope fractionation (Fig. 2a). Low- $\delta^{18}\text{O}$ rocks and magmas result from high-temperature interaction with, or subsequent re-melting of, materials that interacted with meteoric waters at high-temperatures involving small isotope fractionations. Data are from both original sources and compilations by Muehlenbachs (1998); Eiler (2001), Valley et al. (2005); Hoefs (2005); Sharp (2006). Selected areas emphasized in this review are shown as open boxes.

et al. 2003). Establishing the equilibrium fractionation factors for igneous minerals is still an active area of experimental research, especially for refractory accessory minerals, for which direct experiments are difficult (e.g., Krylov et al. 2002; Valley et al. 2003; Trail et al. 2008).

For isotopic fractionation between minerals and melt, most variation is caused by the changing composition of melt. In an attempt to quantify the mineral-melt fractionation factors, the easiest approach is to treat the melt as a mixture of normative minerals and then calculate the weighted average of individual mineral-melt (normative sum) fractionation factors (Matthews et al. 1994; Palin et al. 1996; Eiler 2001; Appora et al. 2002). Although the natural silicate melts are more complicated mixtures of various components those chemical variations are often treated by a regular solution model (Ghiorso and Sack 1995), for the purpose of isotope

fractionation, non idealities of melt mixing functions play a minor role. The normative mineral approach assumes that a normative mineral in melt has the same partition function ratios for isotope distribution; it has been demonstrated to be largely correct assumption for a variety of quartzofeldspathic mixtures, despite a few tenths of one permil disagreement between crystalline quartz and quartz-melt as measured in experiments (Matthews et al. 1998).

When $\delta^{18}\text{O}$ values are relatively similar and not extremely low or high in $\delta^{18}\text{O}$, the fractionation factor $1000\ln\alpha$ is numerically very close to the simple difference between measured $\delta^{18}\text{O}$ values, or $\Delta^{18}\text{O}$ (e.g., Hoefs 2005; Sharp 2006):

$$1000\ln\alpha_{\text{Quartz-Zircon}} \approx \Delta^{18}\text{O}_{\text{Quartz-Zircon}} = \delta^{18}\text{O}_{\text{Quartz}} - \delta^{18}\text{O}_{\text{Zircon}} \quad (3)$$

Isotope fractionation of oxygen between coexisting minerals, like any other stable isotope, is a strong function of temperature; for solid substances at temperatures higher than $\sim 50\text{--}100^\circ\text{C}$, the isotope fractionation factor $1000\ln\alpha$ is a linear function of $1/T^2$ (Biegelsen and Meyer 1947; Urey 1947). The reverse quadratic rather than $1/T$ dependence that is common in thermodynamics of element partitioning is explained by the fact that the factor that causes isotope fractionations— isotope vibrational frequencies, are themselves increasing with temperature. Figure 2 presents isotope fractionations between major igneous minerals and water as a function of T . Note that isotope fractionations are largely pressure-independent for common upper mantle-crustal pressures because isotope substitutions do not have significant volume effects. In $1000\ln\alpha$ vs. $1/T^2$, isotope exchange between minerals, and most likely minerals and silicate melt, can be described by a single A factor:

$$1000\ln\alpha = 10^6 A/T^2 \quad (4)$$

defining linear dependence passing through the origin at infinite temperature at which isotope fractionations are zero.

Because of the reverse quadratic relationship between $1000\ln\alpha$ and temperature (Fig. 2) isotope fractionations between coexisting minerals, melts and fluids are small at high magmatic temperatures, typically less than 2-3‰. It underlies the importance of high precision, better than 0.1‰, to resolve subtle isotopic differences between different sources for magmas. Small (1-2‰) isotope fractionation between minerals were traditionally used to predict that isotope fractionation are consistent with magmatic temperatures and not with subsolidus exchange (e.g., Taylor 1986), meaning that they reflect primary sources rather than secondary isotope effects.

Isotope thermometry. An important aspect of oxygen isotope analysis of coexisting mineral assemblages is the ability to use the experimentally-determined A factors and measured $\Delta^{18}\text{O}$ as input parameters to calculate temperature in Equation (4). Temperature estimates are more easily determined for mineral pairs with large A factors such as quartz and magnetite (Fig. 2B). Several assumptions should be evaluated in order for isotope thermometry to reflect primary magmatic values. First, minerals should be fresh and unaltered, as can be demonstrated under an electron microscope. Second, the rock or magma should have cooled rapidly so that the measured isotope temperature reflects quenched pre-eruptive conditions and does not reflect the effects of slow plutonic cooling with sequential mineral closure to isotope exchange (e.g., Eiler et al. 1993; Farquhar et al. 1993). Third, minerals should be phenocrysts and not isotopically-distinct xenocrysts.

Because the first two conditions are rarely met for metamorphic and likewise plutonic rocks, the initial optimism to be able to use pressure-independent oxygen isotope thermometry (where P and T can be correlative based on chemical geothermometers and geobarometers) nearly disappeared, except for simplest biminerale assemblages involving refractory accessory phases where possibility for exchange is limited (e.g., Valley 2001). However, for fresh volcanic rocks that quenched rapidly, measured $\Delta^{18}\text{O}$ values can be used to determine preeruptive temperature. Young pyroclastic volcanic rocks such as single pumice or tephra

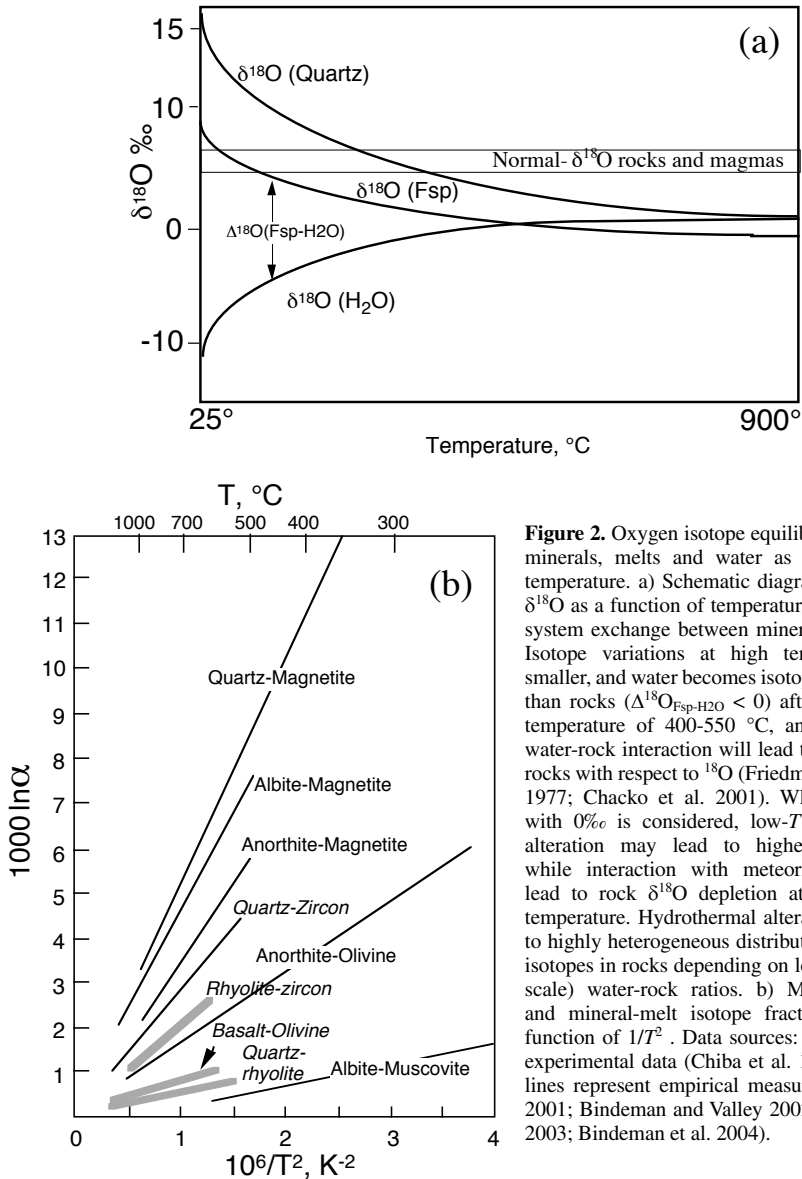
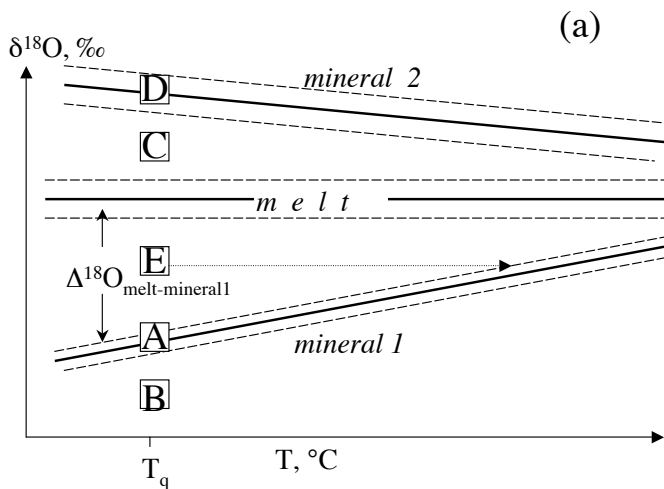


Figure 2. Oxygen isotope equilibrium between minerals, melts and water as a function of temperature. a) Schematic diagram illustrating $\delta^{18}\text{O}$ as a function of temperature for a closed-system exchange between minerals and water. Isotope variations at high temperature are smaller, and water becomes isotopically heavier than rocks ($\Delta^{18}\text{O}_{\text{Fsp-H}_2\text{O}} < 0$) after a crossover temperature of 400-550 °C, and that high- T water-rock interaction will lead to depletion of rocks with respect to ^{18}O (Friedman and O'Neil 1977; Chacko et al. 2001). When sea water with 0‰ is considered, low- T hydrothermal alteration may lead to higher- $\delta^{18}\text{O}$ values while interaction with meteoric water will lead to rock $\delta^{18}\text{O}$ depletion at nearly every temperature. Hydrothermal alteration will lead to highly heterogeneous distribution of oxygen isotopes in rocks depending on local (i.e., mm-scale) water-rock ratios. b) Mineral-mineral and mineral-melt isotope fractionation as a function of $1/T^2$. Data sources: Thin lines are experimental data (Chiba et al. 1989). Thicker lines represent empirical measurements (Eiler 2001; Bindeman and Valley 2002; Valley et al. 2003; Bindeman et al. 2004).

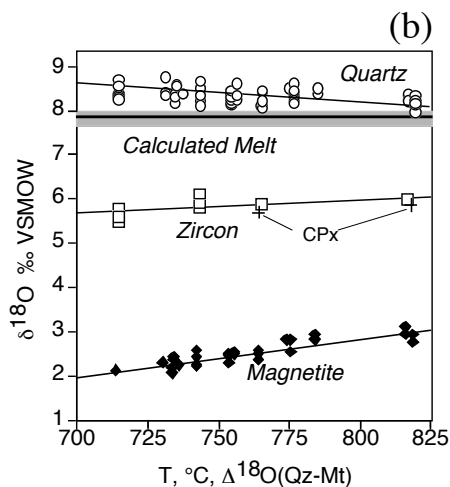
clasts perhaps present the best examples of quenched eruptive products that preserve magmatic $\Delta^{18}\text{O}$ values, and thus temperatures (e.g., Bindeman and Valley 2002, Fig. 3).

Mineral vs. whole rock analysis. Oxygen isotope ratios are used in much the same way as radiogenic isotopes or trace elemental ratios to define or identify different geochemical reservoirs or sources of magmas. In this sense, whole rock oxygen isotope analysis should theoretically represent magma and its source, and such analysis was a common practice in early studies. The early investigation of oxygen isotopes in igneous rocks relied on whole rock analysis by conventional methods; however, large oxygen isotopic variations put forward by



(a)

Figure 3. a) Recognition of $\Delta^{18}\text{O}_{\text{melt-mineral}}$ isotope equilibria and disequilibria. With decreasing temperature, isotope fractionations (divergent lines) between minerals (letter boxes) and melt increase up until the temperature of eruptive quench, T_q , oxygen diffusion is expected to operate without closure. Crystal A (mineral 1) and crystal D (mineral 2) are in isotope equilibrium among themselves and the melt, while individual crystals E, B and C of mineral 1 record disequilibrium $\Delta^{18}\text{O}_{\text{melt-mineral}}$ values. Crystal B comes from a lower- $\delta^{18}\text{O}$ source,



(b)

while crystal C comes from a higher- $\delta^{18}\text{O}$ source, and they are therefore xenocrysts. Crystal E is only subtly, by a few tenths of one permil, heavier than the equilibrium value, and can be interpreted to represent crystallization at higher-temperatures and then capture into a lower-temperature magma differentiate similar to cumulate entrapment. Crystal E could be a “proto”- or “ante” cryst. b) An example of isotope equilibria among minerals and melt in Bishop tuff, a large volume rhyolite deposit in which individual pumice clasts record equilibrium $\Delta^{18}\text{O}_{\text{melt-mineral}}$ isotope fractionations, divergent with decreasing temperature (from Bindeman and Valley 2002). Each vertical column of symbols represent analyses from a single pumice clast erupted from different depth of the thermally-zoned magma chamber ranging from 6 to 11 km (Wallace et al. 1999) thus quenching specific magmatic $\Delta^{18}\text{O}_{\text{melt-mineral}}$ values. The obtained isotopic temperatures agree very well with Fe-Ti oxide temperatures in the Bishop tuff clasts.

these early researchers were later reinterpreted as being mostly due to secondary alteration effects with surface waters (Taylor 1986). Studies of minerals instead of rocks, and in particular refractory phenocrysts such as quartz, zircon and olivine, yielded a picture of subtle subpermil variations in $\delta^{18}\text{O}$ within the mantle (Valley et al. 1998; Eiler 2001) and narrower ranges in many crustal rocks (e.g., Valley et al. 2005). Fresh glass of modern or recent volcanic rocks that is unaltered can be used to directly infer primary magmatic $\delta^{18}\text{O}$ values. However, volcanic glass in old rocks is metastable and exchanges oxygen with waters even before there is clear petrographic evidence of devitrification or development of microscopic clays (e.g., Taylor 1986). Iridescence in sanidine and glass, which may signal the appearance of microscopic clays can be used as an indicator of $\delta^{18}\text{O}$ modification.

Unaltered phenocrysts in igneous rocks provide a better view of true magmatic $\delta^{18}\text{O}$ value, but they are different from the $\delta^{18}\text{O}$ value of the magma by a fractionation factor $\Delta^{18}\text{O}_{\text{mineral-melt}}$ that is a function of temperature, melt composition, and, for the case of plagioclase and similar heterovalent solid solution, their Ca/Na and Al/Si ratios. In studies involving comparison of $\delta^{18}\text{O}$ between different magmas or sections in a drillcore, it is better to present data for a single

mineral if possible (e.g., Wang et al. 2003). In some other applications, a calculated magma value can be generated and compared, especially if $\delta^{18}\text{O}$ values of multiple phenocrysts are obtained. Additionally, when relying on $\delta^{18}\text{O}$ values of crystals in old volcanic or plutonic rocks, it is better to avoid feldspars and micas, and rely on “refractory” phases that are resistant to secondary isotope exchange, and do not have solid solution that fractionates oxygen isotopes. For that matter, quartz and zircon in silicic rocks, and olivine in basic rocks, provide reliable proxies for their parental melts, while plagioclase and K-feldspar are less reliable.

The use of phenocrysts requires extra time for mineral separation—a task that was tedious for conventional resistance-furnace fluorination that necessitates 5–25 mg of monomineralic separate. With the reduction of sample size by ten-fold, mineral separation time is now trivial or minimal for laser fluorination and ion microprobe methods. This translates into better quality, inclusion-free, alteration-free separate. Most importantly, the 0.5–2 mg typical sample size for the laser fluorination analysis overlaps with sizes of typical phenocrysts of most rock-forming minerals, thus allowing them to be studied individually, an approach utilized in this Chapter.

Oxygen isotopes in mantle-derived rocks, normal- $\delta^{18}\text{O}$, high- $\delta^{18}\text{O}$, and low- $\delta^{18}\text{O}$ magmas

Basaltic magmas of mid-ocean ridges and most common island arc basalt are characterized by a relatively narrow $5.7 \pm 0.2\text{‰}$ range of $\delta^{18}\text{O}$ values calculated from phenocrysts or measured directly in fresh glasses (Fig. 1). The OIB basalts document greater range of +4 to +6‰ and reflect recycling of materials that interacted with surface waters at low or high temperature into the mantle (Fig. 1). Eclogite nodules and serpentized ultramafic rocks exposed on the surface document greater $\delta^{18}\text{O}$ ranges (Kyser et al. 1982; Harmon and Hoefs 1995). High- $\delta^{18}\text{O}$ magmatic values are seen in intermediate and silicic rocks in continental arcs and collision zones, in magmas that were derived from or interacted with metasedimentary protoliths; low- $\delta^{18}\text{O}$ values characterize caldera settings and rift zones that involve shallow crustal recycling of rocks interacted with meteoric waters at high- T . Reviews by Taylor (1986) and recent reviews by Eiler (2001) and Valley et al. (2005) provide a comprehensive account of whole-rock and phenocryst-based oxygen isotope geochemistry of the mantle and the crust. This chapter challenges these studies somewhat by documenting new complexity revealed by individual phenocryst studies, which shows far greater ranges in individual phenocryst $\delta^{18}\text{O}$ values that reflect crystallization from or exchange with the diverse melts (open boxes in Fig. 1).

It is convenient to define most common basic magma as “normal- $\delta^{18}\text{O}$ ” and consider products of its differentiation-crystallization as a “normal- $\delta^{18}\text{O}$ differentiation array” (Fig. 4). It has been noted in many natural examples of closed-system differentiation series that differentiation of basalt leads to a small subpermil increase in $\delta^{18}\text{O}$ melt value, with a particular magnitude and trajectory of increase weakly dependent on the sequence of phase appearances that affect $\Delta^{18}\text{O}_{\text{mineral-melt}}$ (Anderson et al. 1971; Taylor and Sheppard 1986; Eiler 2001).

In order to better understand mineral-melt oxygen isotope partitioning, and calculate basaltic magma differentiation trends based on experimental mineral-mineral and mineral-melt partitioning, a computational approach can be taken. The rich existing database on mineral-mineral isotope fractionation (Friedman and O’Neil 1977; Chiba et al. 1989; Chacko et al. 2001, and others), is now complemented by isotope exchange experiments involving CO_2 gas as an exchange medium and silicate melts of variable composition (see summary in Eiler 2001). We recommend continuing with the practice of treating melt as a mixture of normative mineral components and calculate $\Delta^{18}\text{O}_{\text{phenocryst-melt}}$ isotope fractionation as a weighed sum of $\Delta^{18}\text{O}_{\text{phenocryst-normative mineral}}$ in melt between the phenocryst and each normative component of the melt for a given temperature. This approach has been used by Eiler (2001) to demonstrate small (<0.2–0.3‰) isotopic differences between variably differentiated basic rocks as a function of basalt MgO content, by Zhao and Zheng (2003) for rocks of variable composition, and by Bindeman et al. (2004) for extended island arc series as a function of SiO_2 . The latter study

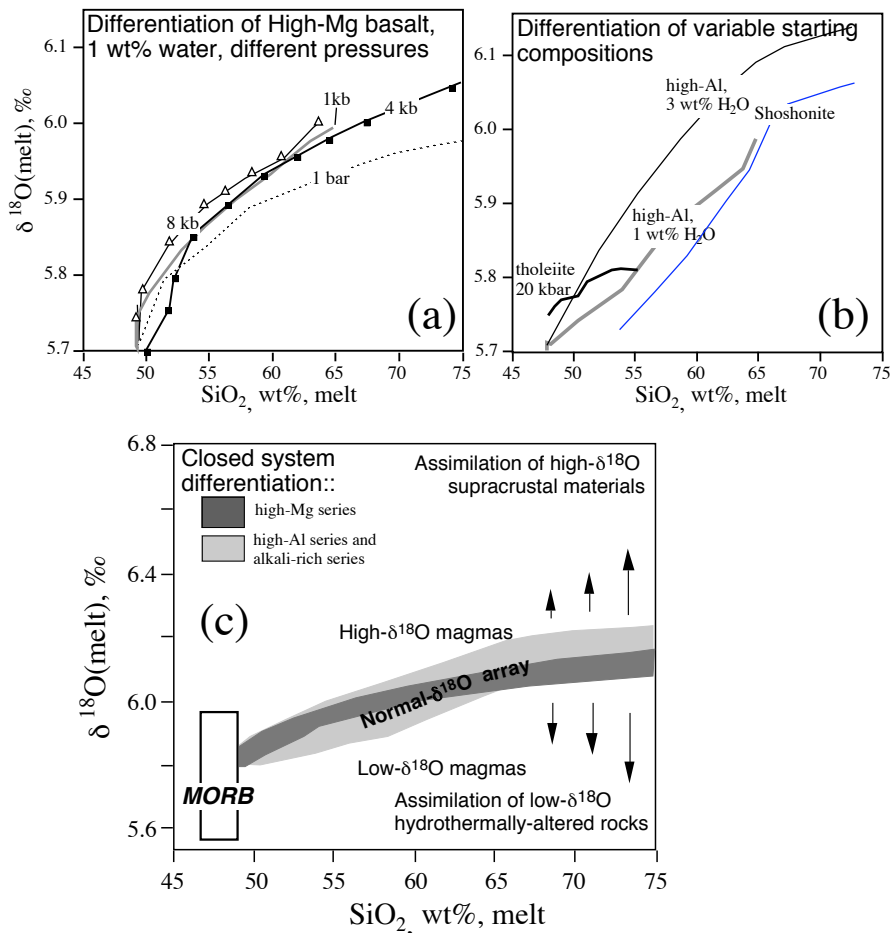


Figure 4. Oxygen isotope effects of closed system igneous differentiation that produce insignificant 0.2-0.5‰ increase and concave-down trend in $\delta^{18}\text{O}$ - SiO_2 coordinates. a) Differentiation of high-Mg basalts in MELTS program at different pressures; b) differentiation of various starting compositions; c) results of multiple numerical crystallization experiments for the two most common island arc series, labeled as “normal- $\delta^{18}\text{O}$ ” magma differentiation array, that separates fields of high- $\delta^{18}\text{O}$ magmas and low- $\delta^{18}\text{O}$ magmas, whose genesis requires open system behavior. After Bindeman et al. (2004).

demonstrated that for a typical igneous rock, a smooth, concave downward trajectory, and an increase of 0.3-0.4‰ is expected in $\delta^{18}\text{O}_{\text{melt}}\text{-SiO}_2$ coordinates from basalt to rhyolite (Fig. 4). Only some rare magmatic series involving unusual Fe-enrichment in the residual melt such as the Skaergaard intrusion yield a nearly flat trajectory (e.g., Anderson et al. 1971; Kalamirides 1984; Bindeman et al. 2008a). A trajectory of $\delta^{18}\text{O}$ increase with SiO_2 is steeper from basalt to andesite because low- $\delta^{18}\text{O}$ minerals such as olivine and pyroxene fractionate early, driving melt toward higher $\delta^{18}\text{O}$ values (Fig. 4). With the appearance of feldspar, the trend flattens while crystallization of near-eutectic quartz+feldspar leads to a nearly constant $\delta^{18}\text{O}$ value of melt and separating cumulate assemblage. The latter is important for high-silica rhyolites that are near-eutectic systems; since the chemical composition of bulk cumulates is the same as the residual melt, the $\Delta^{18}\text{O}_{\text{cumulate-melt}}$ fractionation is zero.

High- $\delta^{18}\text{O}$ magmas. The $\delta^{18}\text{O}$ value of crustal rocks is diverse (Fig. 1, 4), and the majority of crustal igneous rocks have $\delta^{18}\text{O}$ values higher than the mantle magma differentiation array. The majority of cases of isotopically-heavy magma values are related to the exchange, or derivation from, a high- $\delta^{18}\text{O}$ metasedimentary silicate rock (such as metapelites, carbonates, or metagreywackes), that originally crystallized from, or exchanged with, sea water at surface temperatures. Oxygen isotopes serve as an important parameter of crustal assimilation and derivation, especially when coupled with other monitors of these processes such as $^{87}\text{Sr}/^{86}\text{Sr}$ isotopes (Taylor 1980, 1986), U-series, and trace elements (Finney et al. 2008).

Low- $\delta^{18}\text{O}$ magmas. A subset of igneous rocks, silicic and basic, that represent remelting, assimilation or exchange with hydrothermally-altered rocks (altered by heated meteoric waters) represent $\delta^{18}\text{O}$ magmas. The low- $\delta^{18}\text{O}$ rocks were earlier known to occur in only a few locations such as Yellowstone and Iceland (e.g., Taylor 1986). The author of this Chapter is a strong believer of far greater abundance of low- $\delta^{18}\text{O}$ magmas than is currently thought both in terms of volume and the number of volcanic units; however, low- $\delta^{18}\text{O}$ magmas are likely underrepresented in pre-Tertiary geologic record because being of shallow genesis they are eroded away.

PART II: SINGLE PHENOCRYST ISOTOPE STUDIES

A recent upsurge in interest in single crystal studies reflects the advent of trace elemental and isotopic microbeam and microdrilling techniques that are suitable for dating and fingerprinting single crystals. These approaches have led to the realization that many, if not most, igneous systems contain isotopically diverse and chemically distinct crystal populations that are “heterogeneous on all scales” (e.g., Dungan and Davidson 2004). Minerals that are found in magmas as “pheno”crysts may not necessarily have crystallized from their host melt and may be “proto”crysts or cumulates that are entrained into the more differentiated host product, “ante”crysts captured from chamber walls that represent prior episode(s) of magmatism in the same place, or “xeno”crysts captured from rocks that are much older and are not related to the current cycle of magmatism. For review of these topics see Ramos and Tepley (2008) of this volume. Collectively, there is a growing consensus that histories of crystals and crystal populations (“crystal cargo”) and their host melt may be decoupled and thus isotope disequilibria may provide insights into the origin of both crystals and magma.

Many examples of isotopic zoning and disequilibria in volcanic phenocrysts, with emphasis on volcanic arcs, have been described, and a small level of residual zoning may in fact characterize the majority of igneous rocks, even in slowly cooled plutonic examples (Tepley and Davidson 2003). Therefore, the presence of isotopically-zoned phenocrysts provides “blessing rather than a curse” into a potentially important record of magma sources and timescales of magmatic processes.

Modern methods of oxygen isotope analysis of crystals

Sizes of typical “pheno”crysts in volcanic rocks are in the 0.5-2 mm scale, with their relative abundance, expressed through crystal size distribution (Fig. 5), an important textural characterization of a rock that is pertinent to the kinetics of its crystallization (Streck 2008; Armenti 2008 and references therein) and crystal inheritance. A certain mass of material is required for a precise single crystal oxygen isotope analysis, and as seen on Figure 6b, the precision of an isotopic measurement decreases with the method and the amount of material available. For example, the quoted 0.5-2mm range corresponds to 0.35 to 22 mg of crystal mass with density 2.8 g/cm³.

The most precise method for oxygen isotope analysis—laser fluorination—was developed in the 1990s (Sharp 1990; Valley et al. 1995). This method relies on fluorination of ~0.3-2 mg material followed by the multiple-cycle analysis of generated micromol quantities of O₂ or

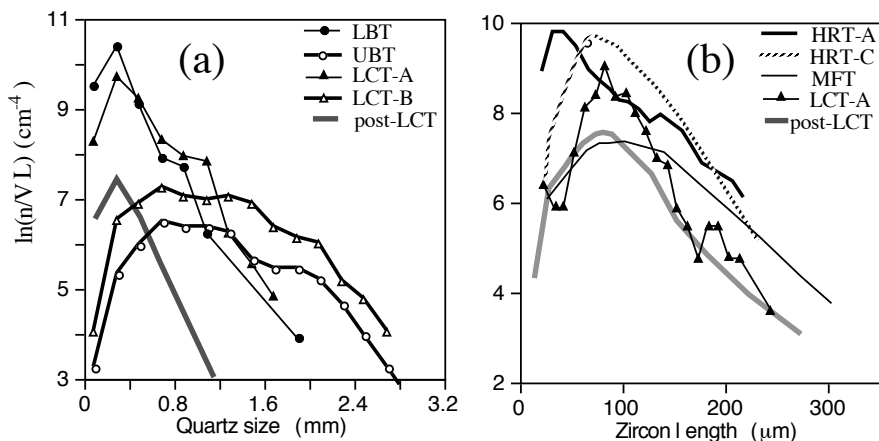


Figure 5. Crystal Size distributions of quartz and zircons in rapidly quenched pumice clasts in large volume tuffs and smaller volume lavas. There are significant differences in crystal sizes and CSD even within the same tuff units. The abundant concave down, lognormal CSDs suggests solution and re-precipitation recycled smaller crystals and the outermost rims of large crystals (e.g., Simakin and Bindeman 2009). CSDs can potentially be used to correlate different magma batches with different crystallization conditions. Abbreviations: HRT- Huckleberry Ridge tuff, LCT- Lava Creet tuff, MFT- Mesa Falls tuff, LBT and UBT are Lower and Upper Bandelier tuffs.

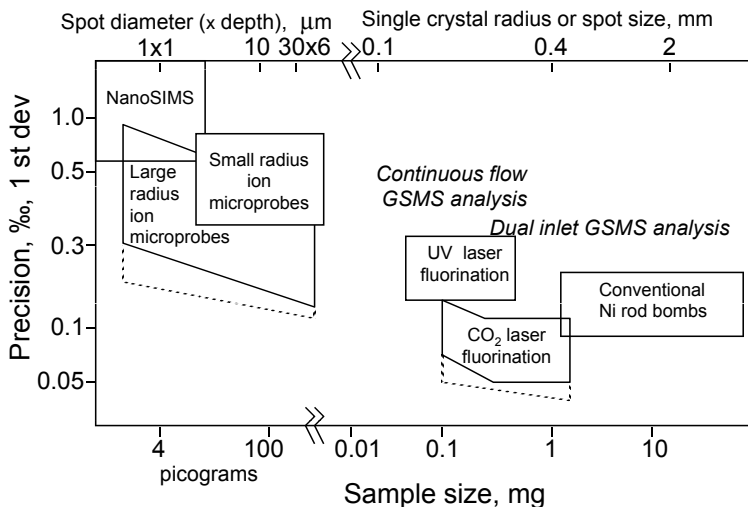


Figure 6. Precision of various analytical methods for oxygen isotopes as a function of sample weight or spot size; precision ranges are current and are based on informed prejudices of the author. Dashed lines represent "best day" precisions.

CO₂ gas on a mass spectrometer against a standard gas of known isotopic composition (dual inlet on Fig. 6). The dual inlet mode of sufficiently large micromol quantities of gas remains the base method of stable isotope mass spectrometry (as TIMS for radiogenic isotopes) analysis with precision improving as a square root of the number of unknown gas-reference gas comparison cycles, commonly better than 0.01-0.02‰ for a typical 6-10 cycle analysis. Most analytical error in oxygen isotope analysis is related to the chemistry of oxygen extraction by fluorination.

Overall external precision in CO₂ laser fluorination labs in Wisconsin, Caltech, and Oregon is “better than 0.1‰” 1 standard deviation, with the uncertainty on standards of ±0.05-0.07‰ common for many analytical sessions (Valley et al. 1995; Eiler 2001; Bindeman et al. 2008c).

The advantage of CO₂ laser fluorination over other methods include: 1) quantitative, 100% reaction of silicate material at temperatures approaching 2000 °C; at such temperatures isotope fractionations between generated gas and potential O-bearing residue are much smaller (ca Fig. 3) than that at 500 °C conventional resistance furnace analysis. 2) High temperature provides the ability to heat and react even the most refractory minerals such as olivine and zircon; 3) reduction of sample size to a single phenocryst that generate enough gas for a multiple cycle, dual inlet analysis. 4) Mineral separation is much less tedious and the quality control is better since it is possible to consistently rely on the highest purity concentrate.

The most important current *in situ* analytical technique for light stable isotopes is ion microprobe analysis. This method uses secondary ions generated by the collision of a primary beam with a target; secondary ions are then analyzed on a mass spectrometer using a variety of secondary ion collection and filtering techniques (Hinton 1995; Ireland 1995; Riciputi et al. 1998; Kita et al. 2004). Spot size can vary from ~2 to 20 μm on large multicollector (e.g., Cameca 1270/80, Page et al. 2007) and small (Cameca 7f) radius ion microprobes, and the analysis time can be remarkably short (6-10 min per spot). However, achieving an appropriate flat polish of the surface to be analyzed and other aspects of sample preparation requirements can be time consuming and challenging. The author’s own use of several large-radius, dual collector instruments yielded external precision of 0.15-0.24‰ on a single spot analysis. NanoSims, an instrument that is used chiefly for nanoscale imaging (e.g., Badro et al. 2007), provides permil precision of submicron particles and areas.

The UV laser fluorination methods (Rumble et al. 1997; Young et al. 1998, 2008) have similar to the ion microprobe precision but greater spot sizes; the advantage of UV laser fluorination is the ability to precisely measure ¹⁷O within single minerals that is important for extra-terrestrial applications (e.g., Young et al. 2008 and references therein).

While CO₂ laser fluorination remains the most precise technique for single crystal isotope studies, the improved techniques of large radius ion microprobe analysis for single spots makes the latter appropriate for studying 1-2‰ level isotope variations required for high-temperature igneous environments. These two methods are likely to complement each other for quite some time in the future.

δ¹⁸O heterogeneity and Δ¹⁸O_{crystal-melt} disequilibria

At equilibrium (Figs. 2-3), a volcanic rock should have consistent δ¹⁸O values of minerals and Δ¹⁸O_{mineral-mineral} and Δ¹⁸O_{mineral-melt} isotope fractionations. However, this chapter documents that examples of isotope disequilibria recognized by single phenocryst isotope studies are more common than previously thought.

Oxygen isotope disequilibria may characterize selected xenocrystic crystals in a population or be the property of the majority of crystals in a rock. The second case clearly requires interpretation of melt and crystal origin in the course of a single petrogenetic process. It is also possible that one mineral may have disequilibrium Δ¹⁸O values while others are in high-temperature equilibrium.

The sign and magnitude of Δ¹⁸O_{crystal-melt} disequilibria may be variable, i.e., magma may be lighter or heavier than the measured or computed values of magma required for equilibrium with each mineral that occurs in it (Fig. 2-3). If a low-δ¹⁸O magma mixes with a high-δ¹⁸O magma, or by assimilating high-δ¹⁸O country rock, the Δ¹⁸O_{crystal-melt} may be small or negative. As an example, magmatic values of refractory minerals that survive slow plutonic cooling, such as zircon and garnet (Lackey et al. 2006), may have a variable sign for the Δ¹⁸O_{mineral-mineral} fractionation.

Petrogenetic processes leading to diverse $\delta^{18}\text{O}$ values and $\Delta^{18}\text{O}_{\text{crystal-melt}}$ disequilibria.

Unlike many radiogenic isotope ratios that can suffer significant changes at <1% addition of isotopically-contrasting component, oxygen is a major element. Modification of $\delta^{18}\text{O}$ value by more than several tenths of 1 permil requires volumetrically-significant mass transformations, by many percents to tens of percent. Such proportions bring mass and heat balance problems to the forefront of the discussion of crystal and magma origins. The following processes are proposed to affect both $\delta^{18}\text{O}$ values, and cause $\Delta^{18}\text{O}_{\text{crystal-melt}}$ disequilibria.

- (i) Interaction with waters or brines derived from country rocks or stopped blocks (e.g., Friedman et al. 1974; Muehlenbachs et al. 1974; Hildreth et al. 1984; Taylor 1986)
- (ii) Rapid assimilation of rocks significantly different in $\delta^{18}\text{O}$ that affects magma and not protocrysts (Taylor 1986; Balsley and Gregory 1998; Spera and Bohrsen 2004).
- (iii) Partial melting of rocks with groundmass that has suffered hydrothermal alteration followed by mixing with more normal magma (e.g., Bacon et al. 1989).
- (iv) Complete or bulk melting of shallow hydrothermally-altered rocks followed by an eruption of magma at the surface (e.g., Bindeman and Valley 2001).

It should be noted that sometimes oxygen isotopic values are the only evidence of petrogenetic processes; this is particularly true when magma exchanges with predecessor rocks of the same chemical or isotopic values (e.g., Bindeman et al. 2008b). Lack of radiogenic ingrowth often renders radiogenic systems to be unable to resolve sources that were in supracrustal environments before being melted (e.g., Lackey et al. 2005). In order to be preserved, transformation of melt $\delta^{18}\text{O}$ that leads to $\Delta^{18}\text{O}_{\text{crystal-melt}}$ disequilibria should proceed faster relative to oxygen diffusive timescales for the largest crystal size, so that reequilibration processes by intracrystalline oxygen diffusion and/or solution-precipitation have not erased the memory of the processes described above. For that matter, volcanic rocks and especially pyroclastic igneous rocks preserve more evidence of disequilibria since volcanic eruption quenches their isotope values (Auer et al. 2008). Fresh tephra, scoria, and pumice clasts may provide the best material to study since they undergo the most rapid cooling, while other volcanic products can suffer post-eruptive growth and reequilibration.

Toward isotopic equilibrium: diffusion vs. solution reprecipitation. It is likely that both intracrystalline diffusion and solution reprecipitation play a role in isotope equilibria. Figures 7 and 11 present two contrasting examples on how to recognize these two processes given intracrystalline zoning patterns. Element mapping, backscatter-electron, and cathodoluminescence imaging are appropriate tools to recognize one from another in the course of isotope investigation. Furthermore, crystal size distribution of minerals aids in deciding the presence or absence of solution-precipitation episodes and on quantifying the amount of material redeposited (Simakin and Bindeman 2008). In particular, abundant lognormal crystal size distributions of zircon and quartz (Fig. 5) suggests that tens of percent of zircon mass was dissolved and reprecipitated, and that the smallest crystals, as well as the rims of the larger crystals, were recycled more than once. The reprecipitation of the rim will not affect the cores of the largest crystals that should retain distinct isotopic values, which are only possible to anneal by intracrystalline diffusion.

Rates of intracrystalline oxygen diffusion vary by 4 orders of magnitude for different minerals (Fig. 8). Increases in oxygen and water fugacity typically decreases oxygen diffusion rates for zircon, olivine, and quartz (Ryerson et al. 1989; Farver and Yund 1991; Watson and Cherniak 1997). Rates of solution reprecipitation are highly variable and depend strongly on the driving forces—undersaturation caused by changes in temperature or composition (e.g., Watson 1996), and are kinetically-limited by the diffusion of the components such as silica through the melt (Zhang et al. 1989). When driving forces for dissolution are great (e.g., at large undersaturations) dissolution may erase evidence of early intracrystalline isotope diffusion and

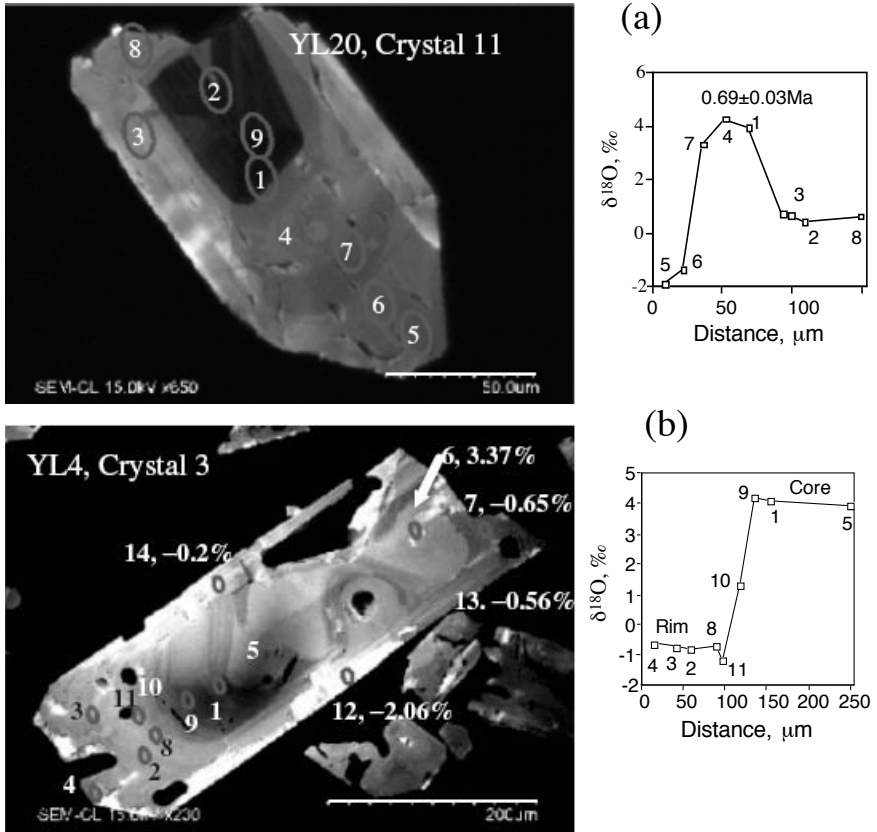


Figure 7. Cathodoluminescence image of isotopically zoned, older zircons from low- $\delta^{18}\text{O}$ rhyolites of Yellowstone and ion microprobe profiles. Sharp boundaries in isotopic composition indicate that solution and re-precipitation in (b) played more important role than intracrystalline diffusion (e.g., bell-shaped profile) in (a). The solution and re-precipitation generated step-function isotope profiles, with higher $\delta^{18}\text{O}$ cores surrounded by the low- $\delta^{18}\text{O}$ rims; faster rates of solution and re-precipitation are capable of erasing the evidence of intracrystalline diffusion. Modified after Bindeman et al. (2008b).

leave sharp boundaries of oxygen isotope distribution within zircon (Fig. 7).

The amount of $\delta^{18}\text{O}$ heterogeneity and the $\Delta^{18}\text{O}_{\text{mineral-melt}}$ disequilibria can be used to predict mineral diffusive timescales if it is assumed that exchange between mineral and melt is rate limited by slow intracrystalline oxygen diffusion. If there is textural evidence that solution-reprecipitation played a more important role in isotope reequilibration, then timescales obtained using diffusion coefficients and intracrystalline diffusion provides the *maximum* time the crystals could have resided in isotopically distinct melt.

PART III: CASE STUDIES OF OXYGEN ISOTOPE DISEQUILIBRIA IN IGNEOUS ROCKS BASED ON SINGLE CRYSTAL ISOTOPE ANALYSIS

Below a review is provided on the examples of oxygen isotope disequilibria found in archetypal examples of basic and silicic magmatism around the world, with emphasize on olivine-basalt, plagioclase-basalt, zircon-rhyolite, and quartz-rhyolite disequilibria that

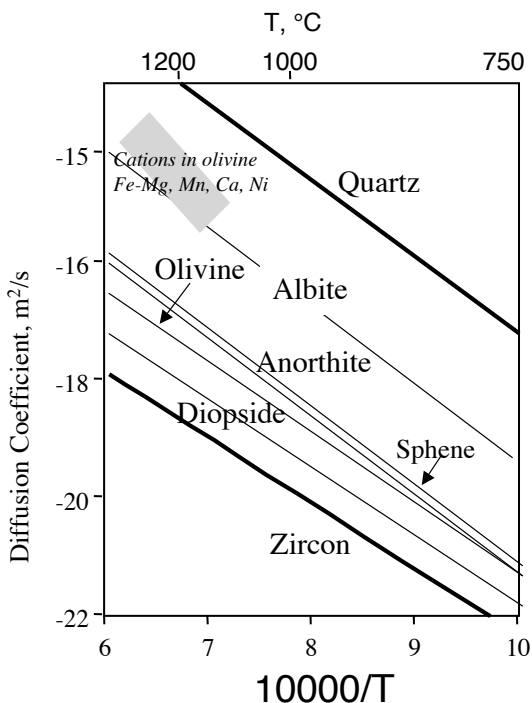


Figure 8. Experimental studies of diffusion with common igneous minerals show four orders of magnitude difference in oxygen diffusion coefficients, and that in olivine cation diffusion is faster than oxygen diffusion. As a result, isotopically-zoned xenocrysts with annealed compositional zoning should be common. Data sources: Zircon, Watson and Cherniak (1997), wet; Sphene, Morishita et al. (1996); Quartz, Farver and Yund (1991), wet; Olivine, Ryerson et al. (1989), QFM; Diopside, Farver (1989); Anorthite and albite, Elphick et al. (1988, 1986) wet.

in $\delta^{18}\text{O}_{\text{melt}}$ from Laki glass. All basalts have exceptionally low- $\delta^{18}\text{O}$ melt value of $3.1 \pm 0.1\%$, homogeneous among 15 km^3 of Laki basalt. This suggests that they tapped a homogeneous and relatively long-lived, well mixed low- $\delta^{18}\text{O}$ magma reservoir that retained its distinct $\delta^{18}\text{O}$ as well as ($^{226}\text{Ra}/^{230}\text{Th}$), ($^{230}\text{Th}/^{232}\text{Th}$), $^{87}\text{Sr}/^{86}\text{Sr}$ and trace elemental values (Sigmarsson et al. 1991). In order to generate such low- $\delta^{18}\text{O}$ value, digestion of tens of percent of low- $\delta^{18}\text{O}$ crust is required.

The preservation of oxygen isotope disequilibria between olivine, melt and plagioclase (Figs. 9, 10) suggests that no more than a hundred years has elapsed since incorporation of plagioclase into basaltic melt because plagioclase has relatively fast oxygen isotope diffusion (Elphick et al. 1986, 1988; Fig. 8). Likewise, time estimates based on mineral diffusive timescales of oxygen and cations in olivine crystals suggests crystal residence for hundreds of years in a well-mixed reservoir under Grimsvötn (e.g., Bindeman et al. 2006b). Similarly short ($<10^2$ yr) time estimates were obtained by Gurenko and Chaussidon (2002) and Gurenko and Sobolev (2006) in their oxygen isotope study of isotopically-zoned olivines from Midfell area.

pertain to the origin of mafic and silicic magmas and their crystals. The examples given here clearly demonstrate the need to explore many more igneous systems for disequilibria relationships, and that single phenocryst isotopic studies of refractory minerals such as olivine and zircon, that can only crystallize from, or exchange with, the high-temperature melt, document the tremendous variety of $\delta^{18}\text{O}$ melts that are present in the crust and the mantle.

Basaltic igneous systems: olivine in basalts

Iceland. The most extreme example of heterogeneous olivine $\delta^{18}\text{O}$ values (3‰ range), and $\Delta^{18}\text{O}_{\text{melt-olivine}}$ and $\Delta^{18}\text{O}_{\text{melt-plagioclase}}$ disequilibria is within the large-volume basalts of Iceland, as described by Bindeman et al. (2006b; 2008c). The greatest 2.2–5.2‰ range of olivine $\delta^{18}\text{O}$ values is measured in the products of 1783–1784AD, 15 km^3 Laki fissure eruption (Fig. 9) and individual plagioclase phenocrysts in the same samples also exhibit disequilibrium relations with olivine and melt. Furthermore, the basaltic tephra erupted over the last 8 centuries and as late as in November 2004 from the Grímsvötn central

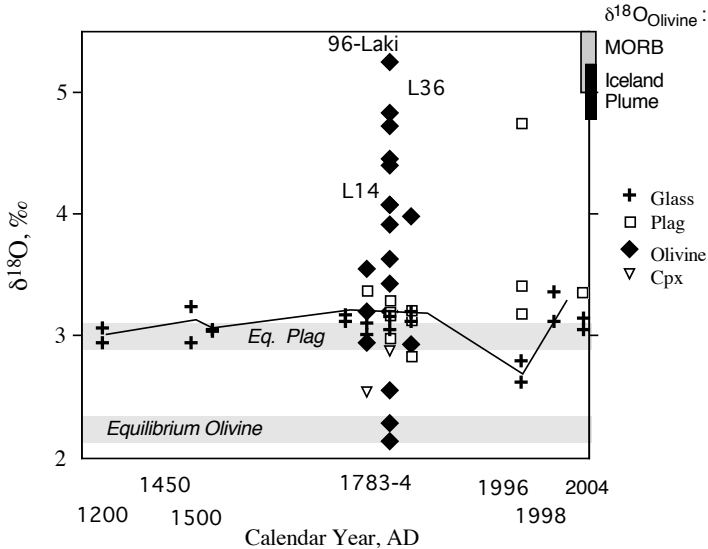


Figure 9. Extreme isotope heterogeneity and disequilibria of individual olivine and plagioclase crystals in the Laki–Grímsvötn magma system based on historical tephra and products of the Laki eruption. There have been relatively constant $\delta^{18}\text{O}_{\text{melt}}$ values for eight centuries and extreme diversity in $\delta^{18}\text{O}$ values of “pheno”crysts. The $\delta^{18}\text{O}$ values of An_{75} plagioclase and olivine in equilibrium with $3.1 \pm 0.1\%$ melt are shown. In the 1996 eruption, plagioclase spans a far wider range than in prior events, which is interpreted here to indicate shorter residence time and later entrainment of feldspars in magma (Bindeman et al. 2006b).

Olivines in other large-volume Holocene basalts of Iceland also display remarkable variety in their $\delta^{18}\text{O}$ and Fe-Mg zoning patterns (Fig. 11). The preservation of Fe-Mg and Ni zoning in some of those olivines suggests that these grains spend less than 100 years in the magma prior to eruption (e.g., Costa and Dungan 2005). Ion microprobe oxygen isotope profiling of single olivine crystals has revealed the presence of crystals that are not zoned but are surrounded by a thin rim (preeruptive xenocrysts); crystals that are zoned with respect to Fe-Mg and $\delta^{18}\text{O}$ (zoned crystals); and crystals that are only zoned with respect to $\delta^{18}\text{O}$ but not composition (compositionally equilibrated, annealed crystals). Moreover, while the majority of crystals have high- $\delta^{18}\text{O}$ cores and low- $\delta^{18}\text{O}$ melt-equilibrated rims, there were a few crystals with the reverse relationship— crystals with high- $\delta^{18}\text{O}$ cores that are diffusively grading into a lower $\delta^{18}\text{O}$ rim, and crystals with relatively abrupt compositional and $\delta^{18}\text{O}$ overgrowth boundaries (Fig. 11). The proportion of “short-residence” zoned crystals with thin overgrowth rims is variable from unit to unit. The majority of crystals in Laki with relatively constant Fo_{75} composition and subtle residual Ni, Ca, Mn zoning requires longer residence (100s of years).

It appears that the best model to explain isotope disequilibria and heterogeneous $\delta^{18}\text{O}$ values in minerals in large volume Holocene basalts from Iceland include magmatic digestion and erosion of Pleistocene hyaloclastites (Bindeman et al. 2008c). Mechanical and thermal magmatic erosion characterizes many lava tubes (Williams et al. 2001, 2004) and it is likely to occur upon basaltic magma flow in the complex network of dikes and sills of the Icelandic rift-related magma plumbing system.

Hawaii. Interesting evidence on $\Delta^{18}\text{O}_{\text{melt-olivine}}$ disequilibria is coming from another classic example of basaltic volcanism—Hawaii. Garcia et al. (1998) analyzed coexisting bulk olivine and matrix glass from the 1983–1997 Puu Oo eruption episode of Kilauea volcano in Hawaii

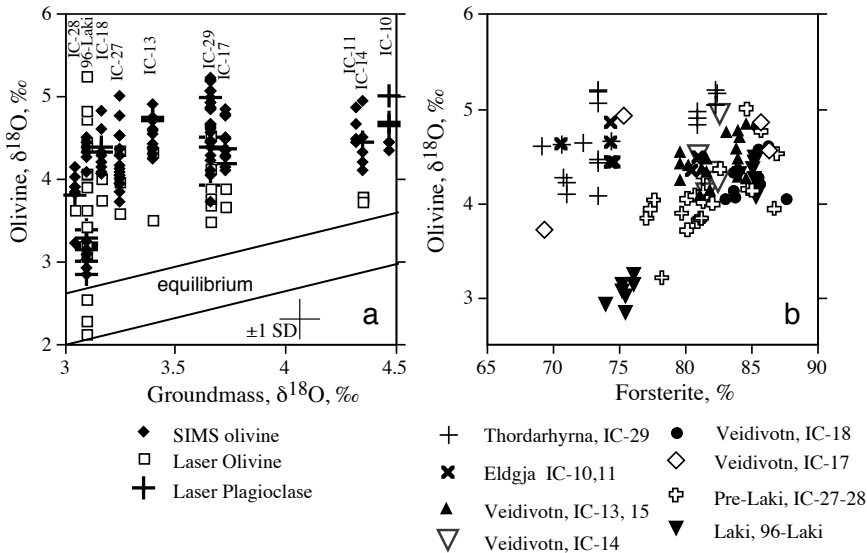


Figure 10. Widespread isotopic heterogeneity of olivine and plagioclase crystals in basalts from Iceland analyzed by laser fluorination and ion microprobe (SIMS). Sample number and corresponding source center are shown; each symbol corresponds to separate lava flow. a) $\delta^{18}\text{O}$ values of glass and olivines vs. $\delta^{18}\text{O}$ value of their host groundmass (measured by laser) arranged by sample (unit) number. Olivines in each sample are lower than the mantle olivine by more than 1‰, and are higher than the expected equilibrium value of olivines with their host groundmass. The field labeled equilibrium denotes $\delta^{18}\text{O}_{\text{olivine}}$ values that would be in equilibrium with their host melt; calculated equilibrium fractionation between olivine and these Icelandic melt compositions of $0.7 \pm 0.3\text{‰}$, defining the range of 0.4–1‰ were obtained using the parameterization of Bindeman et al. (2004). b) $\delta^{18}\text{O}$ values vs. forsterite content of olivines analyzed by ion microprobe and electron microprobe in the same spot. Average standard deviation (± 1 SD) on single spot analysis by the ion microprobe are $\pm 0.24\text{‰}$, and $\pm 0.1\text{‰}$ by the laser fluorination. There is a positive correlation of $\delta^{18}\text{O}$ vs. %Fo for some, while in others there is a distinct bimodal distribution. From Bindeman et al. (2008c).

and observed moderate $\Delta^{18}\text{O}_{\text{melt-olivine}}$ disequilibria deviating by up to 0.8‰ from the estimated equilibria $\Delta^{18}\text{O}_{\text{melt-olivine}} = 0.7 \pm 0.1\text{‰}$ (Fig. 12a). The majority of variation characterizes glass that is too light for rather constant $\delta^{18}\text{O}_{\text{olivine}}$ values. Both olivine and matrix glass in this prolonged eruption are variably depleted by 0.3–0.8‰ relative to the normal mantle and thus require assimilation or exchange with low- $\delta^{18}\text{O}$ hydrothermally-altered rocks inside the Kilauea edifice. It appears that little or no correlation exists between radiogenic isotopes, trace element ratios and oxygen isotope parameters with the exception that late erupted, more magnesian basalts of the Puu Oo eruption were closer to mantle $\delta^{18}\text{O}$ values and had smaller $\Delta^{18}\text{O}_{\text{melt-olivine}}$ disequilibria. Garcia et al. (1998) noticed that the lavas that traveled in the shallow, near horizontal, magma pathways for longer periods of time (Fig. 12b) exhibited greater levels of depletion and $\Delta^{18}\text{O}_{\text{melt-olivine}}$ disequilibria. Although these authors had difficulties finding the right mass balance or a particular mechanism of $^{18}\text{O}/^{16}\text{O}$ pre-eruptive exchange, the fact that variable $\Delta^{18}\text{O}_{\text{melt-olivine}}$ and $\delta^{18}\text{O}_{\text{melt}}$ values occurred in the same eruption limits the timescale of magma-rock interaction to a duration of pre-eruptive residence, of months to years.

In a subsequent study of the Kilauea volcanic record, Garcia et al. (2008) described even larger variability in $\Delta^{18}\text{O}_{\text{melt-olivine}}$ and $\delta^{18}\text{O}_{\text{melt}}$ values in products of 1650–2000AD historic eruptions from Kilauea summit. In contrast to the Grimsvotn-Laki system described by Bindeman et al. (2006b), the Hawaiian record indicated variable $\delta^{18}\text{O}_{\text{melt}}$ values and relatively constant $\delta^{18}\text{O}_{\text{olivine}}$ values that led Garcia et al. (2008) to suggest that melt depletion happened

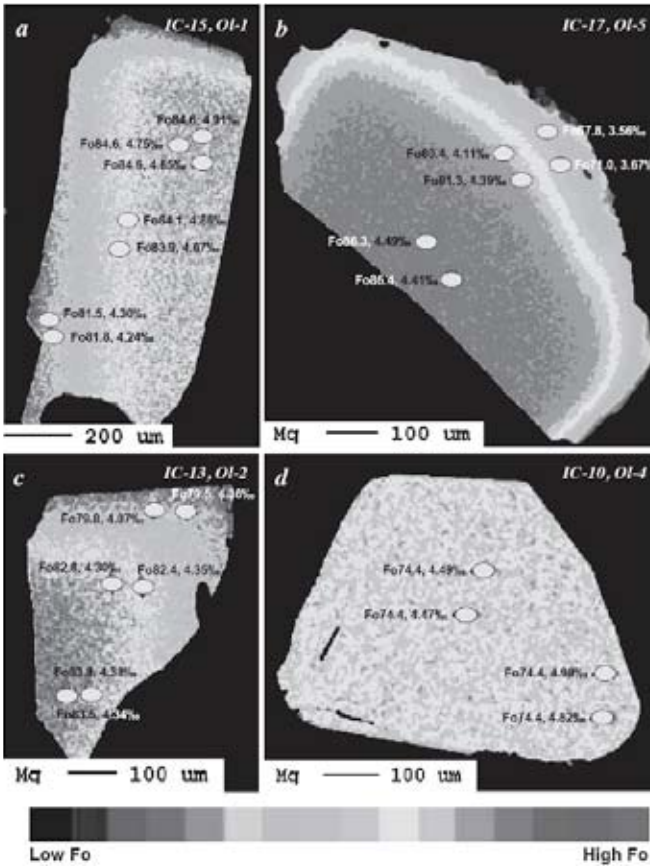


Figure 11. Mg- elemental maps showing various types of elemental and isotopic zoning in olivines from large-volume basalts from Iceland (Bindeman et al. 2008c). Ovals are pits left after ion microprobe analyses of O isotopes. (a-b) grains with normal compositional and isotopic zoning with decreasing Fo and $\delta^{18}\text{O}$ toward the rim; (c) grain with compositional zoning but without isotope zoning; (d) compositionally unzoned grain with subtle increase in $\delta^{18}\text{O}$ toward the rim. [Used with permission of Oxford University Press from Garcia et al. (1998) *Journal of Petrology*, Vol. 39, p. 803-817.]

after olivine grew, perhaps shortly pre- or syn-eruptively (Fig. 12b), and that the difference between Kilauea and Grimsvotn is related to the much smaller magma chamber under the former. There appears to be a correlation of $\delta^{18}\text{O}_{\text{melt}}$ with Pb and Sr isotopes of hydrothermally-altered more radiogenic Mauna Loa lavas, and thus they may serve as a viable assimilate for historic Kilauea lavas.

Isotopically homogenous olivines in Kilauea provide a nice natural analogue to constrain rates of oxygen exchange in olivine. This example suggests that days to months of residence of originally normal- $\delta^{18}\text{O}$ olivines in low- $\delta^{18}\text{O}$ melt was insufficient to cause heterogeneous $\delta^{18}\text{O}$ values in olivine. The examples of large volume basalts from Iceland excluding Laki (Figs. 10-11) continue the trend of exchange and demonstrate that longer olivine residence time in these basalt has led to olivines acquiring low- $\delta^{18}\text{O}$ values and preserving $\delta^{18}\text{O}$ heterogeneity. In Laki, the maximum $\delta^{18}\text{O}_{\text{olivine}}$ heterogeneity and $\Delta^{18}\text{O}_{\text{olivine-melt}}$ disequilibria indicate the longest residence of hundreds of years (e.g., Bindeman et al. 2006b).

Kamchatka. In a study of olivine-matrix relationship of Klyuchevskoy volcano in Kamchatka, the largest in Eurasia, Auer et al. (2008) found a large $\Delta^{18}\text{O}_{\text{melt-olivine}}$ range (Fig. 13) with both positive and negative deviations from equilibrium. Unlike Hawaii and Iceland with low- $\delta^{18}\text{O}$ values, the prolific and tall Klyuchevskoy volcano displays the highest known $\delta^{18}\text{O}_{\text{olivine}}$ and $\delta^{18}\text{O}_{\text{melt}}$ values (Dorendorf et al. 2000; Auer et al. 2008). While most magmas in Klyuchevskoy and the surrounding Central Kamchatka Depression area are high-

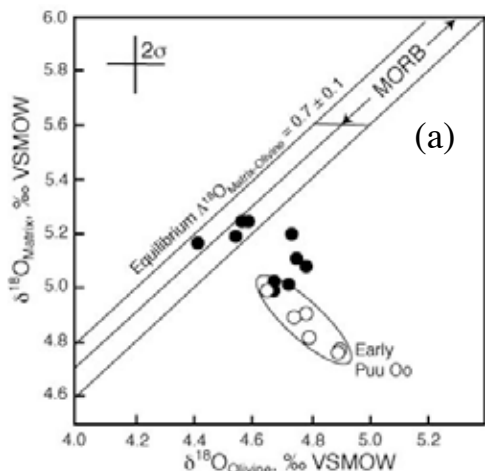
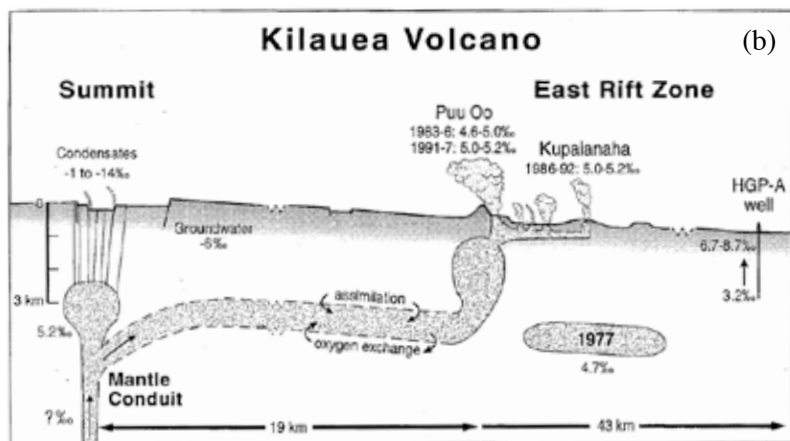


Figure 12. Olivine-Matrix disequilibria in products of Kilauea eruptions. a) Disequilibria in 1983-1997 Puu Oo eruption. b) Magma pathways within Kilauea volcano. [Used by permission of Oxford University Press from Garcia et al. (1998), *J Petrol*, Vol. 38, Fig. 1, p. 805.]



$\delta^{18}\text{O}$ (Portnyagin et al. 2007), the Mg rich component is more normal- $\delta^{18}\text{O}$, while high-Al basalts exhibit the highest $\delta^{18}\text{O}_{\text{olivine}}$ values of 7.6‰. Both high-Mg and high-Al basalt are hydrous with up to 7 wt% water in Fo_{80} melt inclusions (Auer et al. 2008).

Given that variable in $\delta^{18}\text{O}$ olivines also exhibit Fe-Mg disequilibria, and given the correlation of $\delta^{18}\text{O}_{\text{olivine}}$ with Al_2O_3 and MgO content of the parental melt, the best explanation for Klyuchevskoy is pre-eruptive mixing between variable $\delta^{18}\text{O}$ cumulates and high-Al and high-Mg basalts, as well as direct magma mixing between high- $\delta^{18}\text{O}$, high-Al, and lower- $\delta^{18}\text{O}$, high-Mg basalts that are observed in several historic eruptions. Isotopic and compositional heterogeneity of Klyuchevskoy basalts (Fig. 13) is explained by the short time of weeks these olivines spend in magma.

Summary. A histogram of $\delta^{18}\text{O}_{\text{olivine}}$ values measured in the samples discussed above (single crystals and bulk of several or size fraction crystals) are plotted in Fig. 14 and compares them with the two previously published compilations of bulk analysis: $\delta^{18}\text{O}_{\text{whole rock}}$ (Harmon and Hoefs 1995, conventional methods), and $\delta^{18}\text{O}_{\text{bulk olivine}}$ values (Eiler 2001, laser fluorination). It can be seen that the single crystal based studies document far greater $\delta^{18}\text{O}$ range than could have possibly been anticipated by bulk analysis of either whole rocks or multi-crystal concentrates. Olivine is a refractory, early-crystallizing, high-temperature phenocryst, and thus the existence

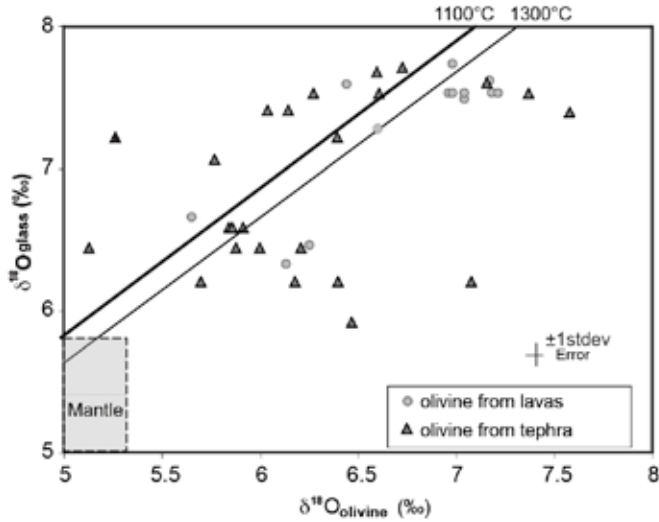
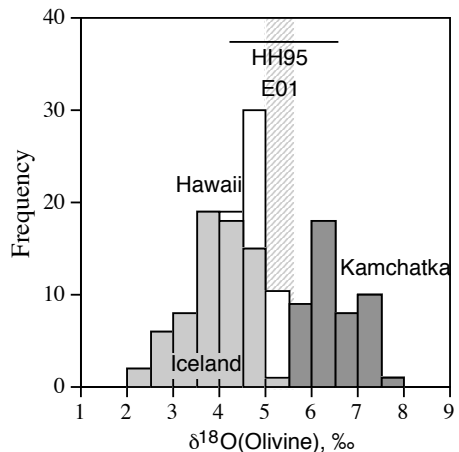


Figure 13. Oxygen isotopic heterogeneity of olivine phenocrysts and their host groundmass for historic or recent (<7 ka) tephra and lava samples from Klyuchevskoy volcano, Kamchatka, Russia. Notice that olivines in a single sample (defined by horizontal arrays) spans up to a few permil to the left and right of equilibrium $\Delta^{18}\text{O}_{\text{olivine-groundmass}}$ values shown by black lines. This extreme $\delta^{18}\text{O}_{\text{olivine}}$ diversity is accompanied by significant Fe-Mg disequilibria between olivine and groundmass. The disequilibria and heterogeneity in this case is explained by short-term pre-eruptive mixing between variable- $\delta^{18}\text{O}$ magma with variable $\delta^{18}\text{O}$ olivines, and by preeruptive mixing between cumulate and magma. From Auer et al. (2008).

Figure 14. Histogram of $\delta^{18}\text{O}$ values of forsteritic olivine measured largely as single phenocrysts in selected examples of basaltic igneous rocks discussed in this work. Hatched pattern marked E01 indicates the majority of olivine values in mantle derived magmas based largely on bulk monomineralic separates summarized by Eiler (2001), while thin horizontal line indicates $\delta^{18}\text{O}$ values of basalt (-0.5 permil for basalt-olivine fractionation) from Harmon and Hoefs (1995). Notice that refractory single olivine records great variety of $\delta^{18}\text{O}$ values of melt from which it crystallized or exchanged with exceeding either laser-based (E01) or conventional, whole-rock values (HH95).



of such heterogeneity demonstrates the existence of basaltic melts either in the mantle or the crust, that span 6‰.

Silicic igneous systems

Isotopic analysis of individual phenocrysts or intra-crystalline domains is a novel tool to fingerprint crystal sources and to recognize separate magma batches of silicic magmas or solid sources from which the crystals once crystallized or were trapped (Tepley et al. 1999; Bindeman and Valley 2001; Wolff and Ramos 2003). Below, we discuss oxygen isotope disequilibria

with the examples of quartz and zircon, two common phases of constant composition and thus simple $\Delta^{18}\text{O}_{\text{mineral-melt}}$ fractionation (e.g., Fig. 3). Zircon has a particular advantage for oxygen isotope studies: it is one of the most refractory, alteration-resistant minerals that retains oxygen isotopic values (Watson 1996; Valley 2003), it is a prime mineral for U-Th-Pb geochronology, and it is a prime mineral for other isotopic (e.g., Hf) and trace elemental studies (Hanchar and Hoskin 2003).

Isotope zoning and Residual memory in Zircon. U-Pb ion microprobe dating of zircon crystallization in volcanic samples demonstrates that zircon crystallization (and closure to subsequent U-Pb exchange) commonly predates the eruption of host lavas as determined by Ar-Ar dating. This has been documented for a range of different sized magma systems. Miller and Wooden (2004) found that zircons in Devils Kitchen rhyolite (Coso volcanic center, California) are up to 200 k.y. older than corresponding K-Ar ages, and several zircon populations with different pre-eruptive histories could be identified, signifying an origin from different magma batches. Simon and Reid (2005) suggested that zircons in the Glass Mountain rhyolites (Long Valley, California) record episodes of punctuated and independent evolution rather than the periodic tapping of a long-lived magma chamber. U-Pb zircon ages in combination with Ar-Ar potassium feldspar ages for the Geysers pluton (California Coast Ranges) indicate that the shallow portions of the pluton cooled to $<350\text{ }^{\circ}\text{C}$ within ~ 200 ka, whereas at the same time zircons from just solidified granitoids at deeper levels became remobilized by the heat of newly intruded magma (Schmitt et al. 2003a,b). Charlier et al. (2005) found zircon ages spanning 100 k.y. in the Taupo volcanic zone in New Zealand, and interpreted zircons to be derived by bulk remobilization of crystal mush and assimilation of metasediment and/or silicic plutonic basement rocks. In their study of Crater Lake volcanic rocks, Bacon and Lowenstern (2005) identified parental rocks as a source for antecrystic zircons and plagioclase in the form of co-erupted granodioritic blocks and magmas. These studies did not reach a universal conclusion on the state of silicic magma bodies in the crust, but favored variably “long” zircon residence in “mushy” upper crustal magma chambers (e.g., Vazquez and Reid 2002; Reid 2003).

Oxygen isotope analysis of U-Pb dated zircon populations provides an important additional insight into the origin of zircons and their host magmas. Many large silicic magma systems display remarkably different degrees of oxygen isotope disequilibria and diversity in their phenocryst populations.

Case studies of large silicic magma systems

Bishop tuff. On one extreme, there is a nearly homogeneous $\delta^{18}\text{O}$ magma body parental to Bishop tuff (Fig. 3b, Bindeman and Valley 2002) in which zircon appears to be in perfect $\Delta^{18}\text{O}$ equilibrium with other minerals; on the other extreme there are rhyolites from Yellowstone, with tremendous diversity in age, $\delta^{18}\text{O}$ and $\Delta^{18}\text{O}_{\text{Zircon-melt}}$ values (Fig. 15). The erupted Bishop tuff magma body was equilibrated with respect to the major element oxygen (Fig. 3b) and did not retain zircon or other phenocrystal evidence of inheritance from the Glass Mountain magmas (Simon and Reid 2005). The pre-Bishop Tuff, Glass Mountain rhyolites, erupted over a time-span exceeding 1 Ma, exhibit heterogeneity with respect to Sr, Nd, Pb, and O isotopes between different domes (Davies and Halliday 1998; Bindeman and Valley 2002; Simon and Reid 2005). Subsequent accretion of these magma batches led to the formation of the Bishop Tuff magma body, which averaged isotopic differences in the melt, equilibrated $\delta^{18}\text{O}$ in minerals, and rejuvenated U-Pb ages of zircons (Reid and Coath 2000). Several other large volume rhyolites: Cerro Galan, Toba, Fish Canyon, both monotonous-intermediates, and high-silica rhyolites, exhibit relative isotope homogeneity between early and late eruption products (Bindeman and Valley 2002).

Yellowstone. On the other end of the spectrum, Yellowstone intracaldera volcanic rocks belonging to the Upper Basin lavas are an example where almost the entire population of zircons is inherited from precaldera source rocks spanning 2 m.y., based on both U-Pb zircon ages and

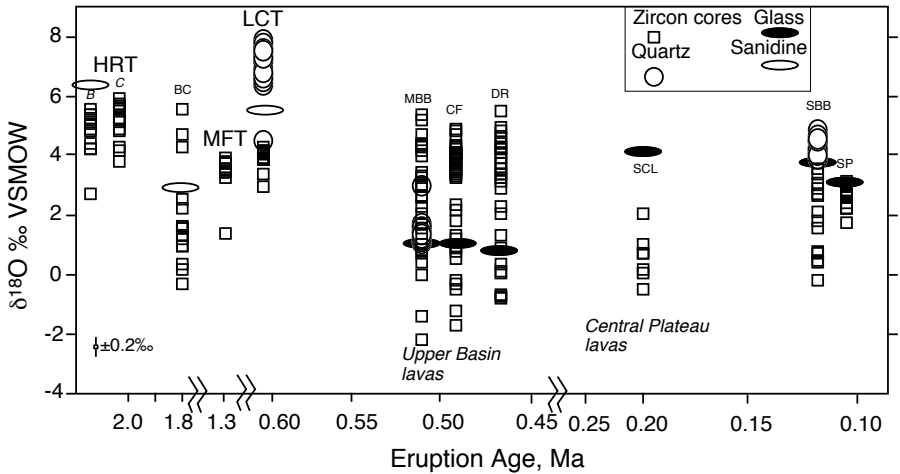


Figure 15. Isotope disequilibria and diversity of $\delta^{18}\text{O}$ values of zircons and quartz from selected rhyolitic lavas and tuffs from Yellowstone Plateau volcanic field, Wyoming, USA measured by the large radius ion microprobe. Analyses of $\delta^{18}\text{O}$ are plotted vs. Ar-Ar eruptive age (Gansecki et al. 1996; Lanphere et al. 2002); the age of the SBB is by U/Th dating of zircon rims, (Watts et al., unpublished data); BC age is by K-Ar (Obradovich (1992). HRT, MFT, and LCT are Huckleberry Ridge (Members B and C), Mesa Falls, and Lava Creek tuff caldera forming eruptions; Unit abbreviations: BC - Blue Creek, MBB and SBB are Middle and South Biscuit Basin, DR- Dunraven Road, SCL- Scaup Lake, SP- Solfatara Plateau. Modified after Bindeman et al. (2008b).

$\delta^{18}\text{O}$ values (Bindeman et al. 2001; 2008b). Tremendous ranges of $\delta^{18}\text{O}$ values of phenocrysts and variable $\Delta^{18}\text{O}_{\text{mineral-melt}}$ and $\Delta^{18}\text{O}_{\text{quartz-zircon}}$ disequilibria in the majority of 6000 km³ volcanic rocks in Yellowstone (Fig. 15) are revealed by individual quartz phenocryst analysis by laser fluorination, and individual zircon analysis by ion microprobe. These rhyolites are the products of nearly wholesale remelting and recycling of hydrothermally altered materials from earlier eruptive cycles, and they preserve extreme oxygen isotopic variability and zoning in phenocrysts, including quartz (Bindeman and Valley 2001).

Timber Mt. Caldera Complex, Nevada. Intermediate between Yellowstone and Long Valley, are the large volume low- $\delta^{18}\text{O}$ Ammonia tanks rhyolites of Timber Mountain caldera in Nevada (Fig. 16) that exhibit $\Delta^{18}\text{O}_{\text{zircon-melt}}$ disequilibria but demonstrate $\Delta^{18}\text{O}_{\text{Quartz-melt}}$ and $\Delta^{18}\text{O}_{\text{Sphene-melt}}$ equilibria. Neither different parts of the large Ammonia Tanks tuff magma body, exemplified by the study of individual pumice clasts dispersed by the caldera-forming eruptions (Mills at al. 1997; Tefend et al. 2007), nor crystal populations, exemplified by the study of phenocrysts (Bindeman et al. 2006a), were unable to achieve whole-rock isotopic and chemical equilibration. Diversity of $\delta^{18}\text{O}$ zircon values in Ammonia Tanks rhyolites is supported by the diversity of their ages that spans the entire history of Timber Mountain caldera complex (Bindeman et al. 2006a).

Recognizing magma batches using individual phenocrysts. At Yellowstone and Timber Mt. caldera complexes, lavas and tuffs with poly-age and diverse $\delta^{18}\text{O}$ zircon populations represent accretion of independent homogenized magma batches that were generated rapidly by remelting of source rocks of various ages and $\delta^{18}\text{O}$ values. Sufficient magma residence time may allow annealing $\delta^{18}\text{O}$ and $\Delta^{18}\text{O}$ values of quartz, then sphene, and then zircon. However, isotope zoning in zircon in these two caldera complexes within even large-volume rhyolites suggest that “residual memory” of accretion and magma derivation from low- $\delta^{18}\text{O}$ hydrothermally-altered rocks has not yet been erased (Fig. 17). Large volume tuffs of Yellowstone and Timber

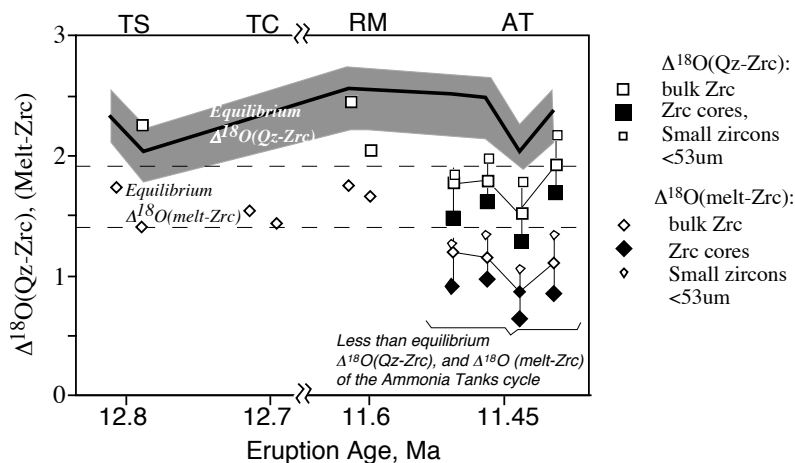


Figure 16. Zircon-quartz and zircon-melt oxygen isotope disequilibria in large volume rhyolites from Timber Mt/Oasis Valley caldera complex, Nevada, using size fraction analysis of zircons by laser fluorination. Large volume units Topopah Spring (TS), Tiva Canyon (TC), and Rainier Mesa (RM) show equilibrium relations, while zircons in all four of Ammonia Tanks (AT) cycle samples have smaller than equilibrium fractionations vs. quartz, due to the inherited high- $\delta^{18}\text{O}$ cores which are present even in smaller zircons; Smaller zircons show closer equilibrium with quartz and melt than larger zircons, because the latter have higher- $\delta^{18}\text{O}$ cores. Spinel and quartz in these samples are in isotopic equilibrium. Four samples in the Ammonia Tanks cycle are plotted in accordance with their relative eruption sequence at around 11.45 Ma. Modified after Bindeman et al. (2006a).

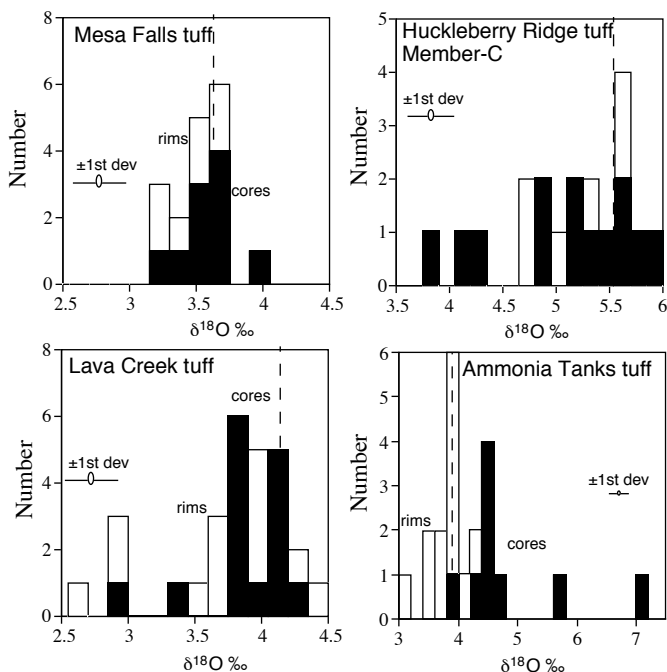


Figure 17. Oxygen isotope diversity and zoning of zircons from major tuff units from Yellowstone and Ammonia Tanks tuff of Timber Mt. caldera complex. Dashed vertical line represents equilibrium value with the host glass. Data from Bindeman et al.. (2006a, 2008b).

Mt. exhibit the $\Delta^{18}\text{O}_{\text{Quartz-melt}}$ equilibria, small $\Delta^{18}\text{O}_{\text{zircon-melt}}$ disequilibria, and diverse $\delta^{18}\text{O}_{\text{zircon}}$ values (Figs. 15-16, Bindeman et al. 2006a, 2008b).

When $\delta^{18}\text{O}_{\text{zircon}}$ values are plotted against the eruptive volume in three large silicic systems (Fig. 18) there appears to be an empirical correlation that suggests decreasing $\Delta^{18}\text{O}_{\text{zircon-melt}}$ disequilibria with increasing volume to $\sim 100\text{-}300\text{ km}^3$. This correlation may indicate that magma bodies of $\sim 100\text{-}300\text{ km}^3$ in size represent well-mixed reservoirs which exist for a long enough time to anneal isotope disequilibria in zircons and other minerals. However, greater heterogeneity that appears in larger, supervolcanic volumes of magma, may reflect late stage or preeruptive magma batch addition or stratification. The only exception from this rule is provided by the Kilgore tuff, 1800 km^3 eruptive unit in the Heise volcanic field in Idaho (Morgan and McIntosh 2005; Bindeman et al. 2007), which appears to have greater homogeneity in zircon age and $\delta^{18}\text{O}$ values.

Phenocryst heterogeneity in plutonic rocks

Plutonic rocks have undergone prolonged cooling that should in theory anneal isotope disequilibria, and evidence of batch segregation given diffusion coefficients and times involved (Fig. 8). However, zircon, a mineral with the slowest oxygen diffusion, demonstrates $\Delta^{18}\text{O}_{\text{zircon-other mineral}}$ disequilibria in studied examples of plutonic rocks. King and Valley (2001) and Lackey et al. (2006) (Fig. 19) studied the oxygen isotopic composition of minerals in the Idaho Batholith and Sierra Nevada Batholith respectively, using two refractory minerals with slow oxygen diffusion—garnet and zircon. At equilibrium, both orthosilicates should have nearly identical $\delta^{18}\text{O}$ values and $\Delta^{18}\text{O}_{\text{zircon-garnet}} = 0 \pm 0.1\text{‰}$ (Valley et al. 2003). King and Valley (2001) and Lackey et al. (2006) observed that near the contact with high- $\delta^{18}\text{O}$ country rocks, zircon retained its average intraplutonic $\delta^{18}\text{O}$ values, while other minerals, including garnet, increased their ^{18}O from the assimilation of high- $\delta^{18}\text{O}$ country rocks. In both examples, lower than equilibrium $\delta^{18}\text{O}$ zircon values, and correspondingly higher than zero $\Delta^{18}\text{O}_{\text{garnet-zircon}}$ values indicated late stage contamination by a high- $\delta^{18}\text{O}$ wallrock that did not affect the previously crystallized zircon. However, it is also possible that their data indicate batch

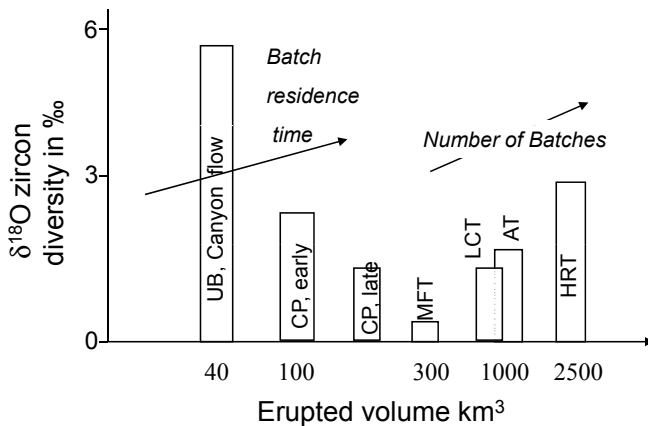


Figure 18. Oxygen isotope diversity of zircons from major tuff units from Yellowstone and Timber Mt. Calderas, and smaller volume rhyolitic lavas as determined by ion microprobe analysis of individual zircons. Achieving isotope equilibrium is interpreted to represent batch residence time that increases with unit size and seems to reach least heterogeneity for units several hundred cubic kilometers erupted as a single cooling unit such as Mesa Falls tuff. More voluminous units develop greater heterogeneity due to the number of erupted Members. Unit abbreviations are the same as in Figures 15 and 16; CP and UB are Central Plateau and Upper Basin post Lava Creek tuff intra-caldera lavas of Yellowstone.

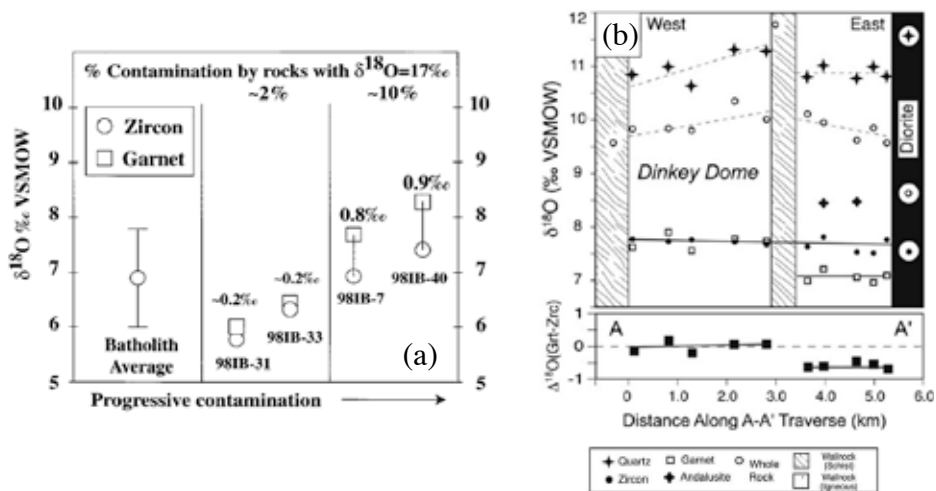


Figure 19. Two examples of plutonic oxygen isotope disequilibria between zircon and other minerals. a) Idaho Batholith (King and Valley 2001) showing progressively divergent $\Delta^{18}\text{O}_{\text{garnet-zircon}}$ fractionation closer to the contact with high $\delta^{18}\text{O}$ country rock; b) Variations in $\delta^{18}\text{O}$ and $\Delta^{18}\text{O}_{\text{garnet-zircon}}$ across Dinkey Dome pluton, Sierra Nevada Batholith. In both examples lower than equilibrium $\delta^{18}\text{O}$ zircon values, and correspondingly greater than zero $\Delta^{18}\text{O}_{\text{garnet-zircon}}$ values indicate late stage contamination by a high- $\delta^{18}\text{O}$ wall-rock that did not affect already crystallized zircon. Equilibrium $\Delta^{18}\text{O}_{\text{garnet-zircon}} = 0$ value is expected to be ~ 0 ‰ (Valley et al. 2003). [Used with kind permission of Springer Science+Business Media from Lackey et al. (2005) *Contrib Mineral Petrol*, Vol. 151, p. 20-44, and King and Valley (2001) *Contrib Mineral Petrol*, Vol. 142, p. 72-88.]

accretion similar to the volcanic examples outlined above: it is noteworthy that $\Delta^{18}\text{O}_{\text{zircon-garnet}}$ disequilibria was only preserved near intrusive contacts because these likely involved intraplutonic quench. Both King and Valley (2001) and Lackey et al. (2006) emphasized slow oxygen diffusion and high closure temperature for zircon, and thus the ability of zircon to retain its original crystallized magmatic value.

In their ion microprobe study of zircons in plutonic rocks, Bolz (2001), Appleby (2008), and Appleby et al. (2008) documented further examples of $\delta^{18}\text{O}$ heterogeneity. The latter paper presents detailed ion microprobe data for zircons in two diorites associated with the Scottish Caledonian Lochnagar pluton. The diorites are very similar with respect to whole-rock chemical composition and age but have very different zircon oxygen isotope compositions. One diorite sample forms a homogeneous zircon population but the other covers a large range of $\delta^{18}\text{O}$ values of several permil. Variations mostly occur between individual zircon crystals, but $\delta^{18}\text{O}$ zoning is also present within a few crystals. While in the majority of cases $\delta^{18}\text{O}$ increases with zircon growth, as is found in the studies of Lackey et al. (2006) and King and Valley (2001), there are individual zircon crystals with the reverse relationship in the same sample, suggesting that several mixing events of variable $\delta^{18}\text{O}$ batches occurred. The same diversity and zoning pattern is also found in a larger sample suite from Lochnagar and Etive plutons (Appleby 2008), and $\delta^{18}\text{O}$ zoning and disequilibria, supported by U-Pb age, differences in Hf isotopic values of zircons, and their REE values, appears to be a common phenomenon in these two plutons.

Summary. Highly diverse $\delta^{18}\text{O}$ zircon values of rhyolites in the examples discussed in this Chapter (Fig. 15 and 17) can be complemented by analyses of $\delta^{18}\text{O}$ values in single zircon and other refractory igneous minerals (see Bolz 2001; Bindeman et al. 2008a,c; Appleby et al. 2008) that demonstrate a picture of diverse silicic magma sources. Since zircons can only

exchange oxygen upon crystallization from melt or through a prolonged exchange with melt, such diverse $\delta^{18}\text{O}_{\text{zircon}}$ values record the diversity of crustal melts that are coming from high- $\delta^{18}\text{O}$ and low- $\delta^{18}\text{O}$ sources and then mix effectively. It is likely that plutons and large volume batholiths are assemble by pulses (Grunder 1995; Davidson et al. 2001; Coleman et al. 2004; Glazner et al. 2004; de Silva and Gosnold 2007) and we now find single crystal isotopic evidence of these assembly processes. The lack of isotope zoning and disequilibria in some large-volume rhyolites such as Bishop tuff (Fig. 3b) suggest convection and annealing due to magma residence and these topics are discussed below.

PART IV: ISOTOPE DISEQUILIBRIA: WHAT HAVE WE LEARNED ABOUT MAGMA GENESIS?

Mineral-diffusive timescales and magma residence times

At high magmatic temperatures, timescales of diffusive equilibration of isotopes and trace elements between crystals and magma are highly variable but are usually short (from <1 to 100s years) relative to magma generation and segregation timescales (e.g., Costa et al. 2008). In this sense, they provide a chronological resolution that is unattainable by most other methods, especially for older rocks in which U-series methods cannot be used (e.g., Bindeman and Valley 2001; Costa et al. 2008). For the youngest volcanic rocks, the age of the melt could be independently constrained by the short-lived U series isotopes, such as ($^{226}\text{Ra}/^{230}\text{Th}$) and ($^{210}\text{Pb}/^{226}\text{Ra}$) activity ratios those half-lives of 1600 yr and 22 yr respectively are comparable with the cation and oxygen diffusion times (Bindeman et al. 2006b; Cooper and Reid 2008). Accessory minerals with slow diffusion coefficients, and particularly zircon (Fig. 8, Watson and Cherniak 1997; Valley 2003) are valuable probes of transient changes by diffusion and solution reprecipitation at high magmatic temperatures, although there appears to be growing evidence that solution-reprecipitation plays a more important role (e.g., Page et al. 2007) and thus diffusion timescales provide maximum time for isotope transformation.

Rapid magma genesis and high magma production rates

The existence of isotopically-zoned and disequilibrium crystals that constitute the majority of crystal populations (Figs. 9, 10, 15, 17) suggests rapid magma genesis. Hundreds to thousands of years time seems reasonable to generate small volume igneous bodies of a few cubic kilometers or less, given average magma production rates in arcs and plumes of 0.001-0.01 km^3/yr (Dufek and Bergantz 2005; McBirney 2006). The remarkable observation which is coming from single crystal isotope studies is that large volume (40-1000 km^3) rhyolites (Figs. 15, 17) and large volume (3-20 km^3) basalts (Figs. 9-13), all have isotope disequilibria for the majority of their crystals. For example, the voluminous 1000 km^3 Ammonia Tanks rhyolite from the Timber Mt. caldera complex demonstrate that individual, isotopically-distinct melt batches generated by reheating of hydrothermally-altered rocks were able to coalesce over time-scales of <150 ky, or likely <10 ka (Fig. 20) into a ~1,000 km^3 size magma body (Mills et al. 1997; Tefend et al. 2007; Bindeman et al. 2006a). In this period of time, hundreds of cubic kilometers of hydrothermally-altered low- $\delta^{18}\text{O}$ protolith were melted and digested, and inherited zircons with older ages and higher- $\delta^{18}\text{O}$ cores survived the hydrothermal alteration and melting. High magma production rates of ~0.01 km^3/yr are thus estimated, which require intrusion of substantial volumes of basaltic magmas on the order of many hundreds of km^3 , that preceded the melting process and may require ignimbrite "flare-up" (e.g., de Silva and Gosnold 2007).

Likewise, in order to generate a Laki-size basaltic flow of 15 km^3 in 1000 to 8000 years based on mineral-diffusive timescales of isotopically-zoned crystal populations, and excess of ($^{226}\text{Ra}/^{230}\text{Th}$), high magma production and accumulation rates of 0.002-0.02 km^3/yr are required. It should also be noted that these are minimum estimates based on the erupted volumes and

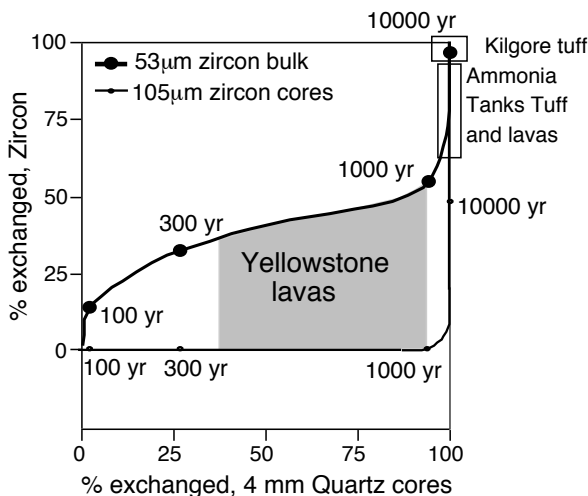


Figure 20. Timescale of magma genesis based on isotope re-equilibration between quartz in zircon within rhyolitic melt at 850 °C using diffusion coefficients from Watson and Cherniak (1997) and Farver et al. (1991), and diffusion in a sphere equation from Crank (1975). A mineral core constitutes the inner 50% of diameter. The field for isotopically-diverse Yellowstone zircons and quartz is shown and requires a 500-5000 yr residence time of xenocrysts in magma. In Ammonia Tanks tuff, quartz $\delta^{18}\text{O}$ zoning is totally annealed, while the remaining subtle 1.5‰ zoning in zircons is consistent with 15,000-20,000 yr of residence at the same conditions. This model predicts that disequilibria due to unequal exchange between quartz and zircon would persist for up to 2000 yr; after that only zircon would show internal zoning lasting for up to ~30,000 yr. Diffusion is assumed to become important when temperatures increase during melting and to stop during eruption. The range of zircon zoning in Ammonia Tanks tuff is consistent with ~10,000 yr from melting to eruption, but for the Kilgore ignimbrite (Heise volcanic field) is longer (Bindeman et al. 2007). The range of zircon and quartz zoning in Yellowstone's low- $\delta^{18}\text{O}$ rhyolites (Bindeman and Valley 2001) and from Timber Mt. (Bindeman et al. 2006b) are consistent with shorter residence times in smaller-volume low- $\delta^{18}\text{O}$ lavas. While this model is based on diffusion, this solution provide maximum timescales if solution and re-precipitation played more important role.

assuming complete evacuation of magma reservoirs and thus could be several times greater if the erupted proportion is only a fraction of the total magma generated. The quoted magma production rates are high but lower than Hawaii's hot spot eruption rates of ~ 0.01-0.1 km³/yr.

Very shallow petrogenesis and the role of hydrothermal carapaces

Abundant low- $\delta^{18}\text{O}$ signatures of crystals that we found in great abundance uniquely fingerprint shallow magma petrogenesis since meteoric water does not penetrate deeper than ~10 km, where the closed porosity in rocks no longer allows low- $\delta^{18}\text{O}$ waters to circulate (e.g., Taylor and Shappard 1986). Caldera settings and rift zone environments facilitate hydrothermal fluid flow and shallow petrogenesis through assimilation of hydrothermally-altered carapace around the magma chambers, which we call "crustal cannibalization." Documented examples of shallow level magma genesis presents significant challenges for heat and mass balance. Mechanically, shallow crustal cannibalization processes may involve reactive bulk assimilation (Dungan and Davidson 2004; Beard et al. 2005) which starts when interstitial melt forms interconnected networks, causing the roofrock to collapse and to disintegrate into individual phenocrysts or crystal clusters. The resulting crystal mush then becomes homogenized by convection. Isotopic diffusion and re-equilibration of crystals will last until the eruptive quench. In this model, magma cannibalizes earlier erupted rocks and the old hydrothermal system that penetrated through them. Self-cannibalization generates a low- $\delta^{18}\text{O}$ component

that lowers the $\delta^{18}\text{O}$ value of the magma. At Yellowstone and Crater Lake, large scale, nearly wholesale melting of hydrothermally altered crust occurred rapidly and effectively enough that a significant portion of the old crust with abundant inherited “antecrysts” of zircons, quartz, and plagioclase (Bacon and Lowenstern 2005; Bindeman et al. 2008b) are preserved in the erupted magmas. Likewise, oxygen isotopic heterogeneity of olivine and plagioclase crystals, and disequilibrium relations between crystals and melt in large volume basaltic eruptions in Iceland and basalts of Kilauea (Figs. 11-12) suggest shallow, sometimes preeruptive modification of basalts in the upper few kilometers of crust.

Abundant evidence of shallow magma petrogenesis contradicts common knowledge that it is easy to generate magma in the middle or lower crust where ambient heat balance around magma bodies prevents rapid heat dissipation. Magma genesis by remelting in shallow environments is aided by: 1) rocks in caldera and rift environments that are pre-heated by prior long-term volcanic activity and subsidence that brings surface-altered rocks down to the underlying heat sources (Fig. 21); 2) erupted rocks are porous, fractured and thus relatively easy to disintegrate by a reactive assimilation processes compared to their plutonic equivalent; 3) shallowly emplaced eruptive products contain abundant volcanic glass which means that no latent heat of fusion is required for their remelting (i.e., melting efficiency is greater for volcanic rocks than for plutonic rocks); 4) shallow volcanic rocks in hydrothermal settings are pre-conditioned and saturated with water that promotes flux melting.

Accretion of large silicic magma bodies

The generation and eruption of silicic magmas continues to present challenges in answering questions about the size and longevity of crustal magma bodies, their physical state as either stagnant, near-solidus cumulate mushes, near-liquidus convecting liquids, or initially solid rocks, and the time and depth of their segregation (e.g., Annen and Sparks 2002; Bachmann and Bergantz 2003, 2004; Dufek and Bergantz 2005; Bindeman et al. 2008b).

The Recycling Machine

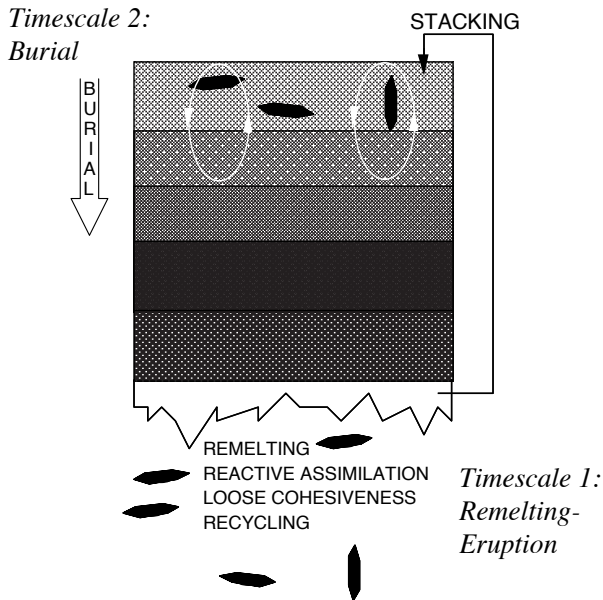


Figure 21. Magmatic cannibalization in shallow crustal environments and timescales of crystal recycling. Progressive burial by caldera collapses, rifting and/or overloading brings erupted volcanic rocks and their sub-volcanic equivalent down deeper to the melting zone. Hydrothermal alteration serves as a flux to cause melting, and glassy, porous nature of these rocks makes re-melting and disaggregation mechanically easier. Timescale 2 is the age between the core and the rim of zircon, while timescale 1 is the crystal diffusive/recrystallization age.

The common theme of documented examples of isotope disequilibria presented in this chapter is batch assembly of magma bodies with initially diverse phenocryst populations, followed by increased mixing and annealing with increased residence time. There is plenty of radiogenic isotope evidence that the accretion of large silicic magma bodies includes batches formed by differentiation of basaltic magmas in the crust, and by partial melting of the radiogenic crust due to heat transport by basaltic intrusions (e.g., see Grunder 1995; Annen and Sparks 2002, and Dufek and Bergantz 2005 for a review of the current literature). Partial melting of the variable- $\delta^{18}\text{O}$ crust will very often generate isotopically-distinct individual magma batches, and isotopes of major element oxygen nicely reflect these processes, especially when constrained by zircons. High- $\delta^{18}\text{O}$ batches reflect supracrustal materials, while low- $\delta^{18}\text{O}$ values document batches that are generated by melting of hydrothermally-altered crustal carapace. Oxygen isotope evidence from the Yellowstone and Timber Mt calderas (Figs. 15-17) indicates that source rocks were cooled below the solidus, altered by heated meteoric waters that imprinted the rocks with low $\delta^{18}\text{O}$ signatures, and then remelted in distinct pockets by intrusion of mafic magmas. Each pocket of new melt was variable in $\delta^{18}\text{O}$, but inherited zircons retained earlier age and $\delta^{18}\text{O}$ values.

The model of remelting and batch accretion presented in this chapter contradicts the commonly held model of a single, large-volume, mushy-state magma chamber that is periodically reactivated and produces rhyolitic off-springs.

The origin of “phenocrysts” and interpretation of their melt inclusions

The presence of $\delta^{18}\text{O}$ zoning and variability among phenocryst populations, as discussed in numerous examples above, suggest that crystals are captured from different $\delta^{18}\text{O}$ sources and thus record different pre-eruptive residence times. For example, phenocryst studies of Icelandic basalts (Figs. 11-12) reveal crystal-scale complexity that requires olivine recycling at different times prior to eruption. The evidence presented above suggests that prolonged annealing and isotopic homogenization of xenocrystic or antecrystic crystal populations is capable of erasing magma memory of crystal origin. Two views on crystal origin are possible: (1) crystals grew from the melt in which they occur, (2) crystals are “annealed beyond recognition” and mixed in with phenocrystic populations that grew from the melt. From the point of view of an isotope geochemist, it is still possible to recognize diverse crystal origins, their fragmentation and recrystallization histories (Fig. 22), and therefore fingerprint magma batches. These annealed crystals may or may not be in chemical equilibria with the host melt and exhibit subtle isotope evidence of diverse sources.

Heterogeneous magmatic origins of olivines in basalts clearly requires the need for reassessment of their melt inclusions, including volatile content (e.g., Thordarson and Self 2003). The same applies to melt inclusion in isotopically annealed quartz or zircon xenocrysts in silicic rocks, which may record melt compositions from previous eruption episodes that predate the host magma by many hundreds thousands years. Melt inclusion compositional studies, combined with identification of melt $\delta^{18}\text{O}$ sources and ages (e.g., melt inclusions in zircon), would provide powerful insights into the chemistry of assembled magma batches.

In this chapter, we presented evidence that annealed crystals are more common than phenocrysts in many basaltic and silicic magma systems around the world. This means that magmas and their crystals cargo may be difficult to produce, but are easy to recycle. Taken as a whole, these results beg the question: are there any “pheno”crysts left?

ACKNOWLEDGMENTS

Author’s prior work with Alfred Anderson, John Valley, John Eiler, and prior and ongoing collaborations with Leonid Perchuk, Olgeir Sigmarsson, Paul Wallace, Vera Ponomareva,

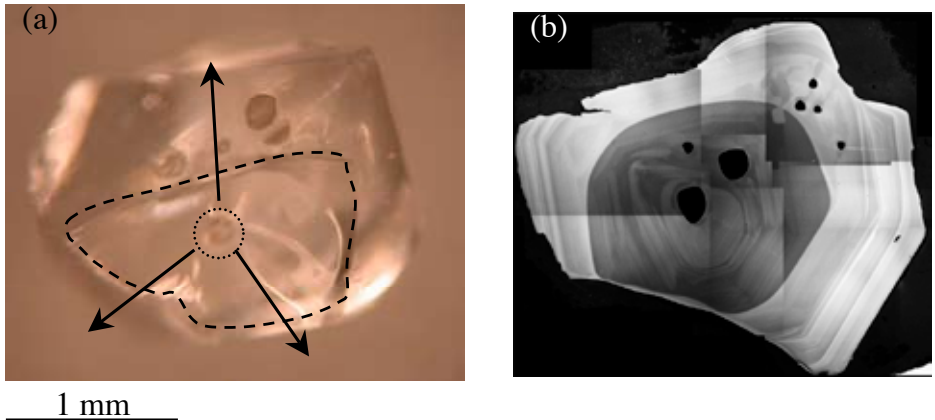


Figure 22. Melt Inclusions in pheno(xeno)crysts: reheated, re-homogenized, decrepitated, and exchanged with the external melt. a) Fragmented host quartz crystal from the Bishop tuff after experimental reheating that lead to melt inclusion decrepitation and fragmentation of crystal. b) Cathodoluminescence image Late Bishop tuff quartz showing sharp boundaries between the dark-CL core and bright-CL rim with melt inclusions in both places (see Wark et al. 2007). Bright CL rims and dark CL cores are nearly identical isotopically (Bindeman and Valley 2002). Image courtesy: Julie Roberge

Axel Schmitt, Andrey Gurenko, and Maxim Portnyagin has led to formulation and maturation of ideas presented here. Informal reviews by Jim Palandri, Erwan Martin, Kathryn Watts, comments by John Valley, and formal reviews by Mike Garcia, Jade Star Lackey, Keith Putirka and an anonymous reviewer have dramatically improved presentation of this chapter. Supported by NSF (EAR0537872) and the University of Oregon.

REFERENCES CITED

- Anderson AT Jr., Clayton RN, Mayeda TK (1971) Oxygen isotope geothermometry of mafic igneous rocks. *J Geol* 79:715-729
- Annen C, Sparks RSJ (2002) Effects of repetitive emplacement of basaltic intrusions on thermal evolution and melt generation in the crust. *Earth Planet Sci Lett* 203:937-955
- Appleby SK (2008) The origin and evolution of granites: an in-situ study of zircons from Scottish Caledonian granites, PhD Dissertation, University of Edinburgh, Scotland
- Appleby SK, Graham CM, Gillespie MR, Hinton RW, Oliver GJH, EIMF (2008) A cryptic record of magma mixing in diorites revealed by high-precision SIMS oxygen isotope analysis of zircons. *Earth Planet Sci Lett* 269:105-117
- Armienti P (2008) Decryption of igneous rock textures: crystal size distribution tools. *Rev Mineral Geochem* 69:623-649
- Auer S, Bindeman I, Wallace P, Ponomareva V, Portnyagin M (2008) The origin of hydrous, high- $\delta^{18}\text{O}$ voluminous volcanism: diverse oxygen isotope values and high magmatic water contents within the volcanic record of Klyuchevskoy volcano, Kamchatka, Russia. *Contrib Mineral Petrol DOI* 10.1007/s00410-008-0330-0
- Bachmann O, Bergantz GW (2003) Rejuvenation of the Fish Canyon magma body: a window into the evolution of a large-volume silicic magma systems. *Geology* 71:789-792
- Bachmann O, Bergantz GW (2004) On the origin of crystal-poor rhyolites: extracted from batholithic mushes *J Petrology* 45:1565-1582
- Bacon CR, Adami LH, Lanphere MA (1989) Direct evidence for the origin of low- $\delta^{18}\text{O}$ silicic magmas: quenched samples of a magma chamber's partially-fused granitoid walls, Crater Lake, Oregon. *Earth Planet Sci Lett* 96:199-208
- Bacon CR, Lowenstern JB (2005) Late Pleistocene granodiorite source for recycled zircon and phenocrysts in rhyodacite lava at Crater Lake Oregon. *Earth Planet Sci Lett* 233:277-293

- Badro J, Ryerson FJ, Weber PK, Ricolleau A, Fallon SJ, Hutcheon ID (2007) Chemical imaging with NanoSIMS: A window into deep-Earth geochemistry. *Earth Planet Sci Lett* 262:543-551
- Baertschi P (1976) Absolute ^{18}O Content of standard mean ocean water. *Earth Planet Sci Lett* 31:341-344
- Balsley SD, Gregory RT (1998) Low- $\delta^{18}\text{O}$ magmas: why they are so rare? *Earth Planet Sci Lett* 162:123-136
- Beard JS, Ragland PC, Crawford ML (2005) Reactive bulk assimilation: A model for crust-mantle mixing in silicic magmas. *Geology* 33:681-684
- Biegelsen J, Mayer MG (1947) Calculation of equilibrium constants for isotope exchange reactions. *J Chem Phys* 15:261-267
- Bindeman IN, Brooks CK, McBirney AR, Taylor HP (2008a) The low- $\delta^{18}\text{O}$, late-stage ferrodiorite magmas in the Skaergaard Intrusion: Result of liquid immiscibility, thermal metamorphism, or meteoric water incorporation into magma? *J Geology*, (in press)
- Bindeman IN, Fu B, Kita N, Valley JW (2008b) Origin and evolution of Yellowstone silicic magmatism based on ion microprobe analysis of isotopically-zoned zircons. *J Petrol* 49:163-193
- Bindeman IN, Gurenko AA, Sigmarsson O, Chaussidon M (2008c) Oxygen isotope heterogeneity and disequilibria of olivine phenocrysts in large volume basalts from Iceland: Evidence for magmatic digestion and erosion of Pleistocene hyaloclastites. *Geochim Cosmochim Acta* doi: 10.1016/j.gca.2008.06.010
- Bindeman IN, Ponomareva VV, Bailey JC, Valley JW (2004) Volcanic arc of Kamchatka: a province with high- $\delta^{18}\text{O}$ magma sources and large-scale $^{18}\text{O}/^{16}\text{O}$ depletion of the upper crust. *Geochim Cosmochim Acta* 68: 841-865
- Bindeman IN, Schmitt AK, Valley JW (2006a) U-Pb zircon geochronology of silicic tuffs from Timber Mt Caldera complex, Nevada: rapid generation of large volume magmas by shallow-level remelting. *Contrib Mineral Petrol* 152:649-665
- Bindeman IN, Sigmarsson O, Eiler JM (2006b) Time constraints on the origin of large volume basalts derived from O-isotope and trace element mineral zoning and U-series disequilibria in the Laki and Grímsvötn volcanic system. *Earth Planet Sci Lett* 245:245-259
- Bindeman IN, Valley JW (2001) Low- $\delta^{18}\text{O}$ rhyolites from Yellowstone: Magmatic evolution based on analyses of zircon and individual phenocrysts. *J Petrol* 42:1491-1517
- Bindeman IN, Valley JW (2002) Oxygen isotope study of Long-Valley magma system: Isotope thermometry and role of convection. *Contrib Mineral Petrol* 144:185-205
- Bindeman IN, Valley JW, Wooden JL, Persing HM (2001) Post-caldera volcanism: In situ measurement of U-Pb age and oxygen isotope ratio in Pleistocene zircons from Yellowstone caldera. *Earth Planet Sci Lett* 189:197-206
- Bindeman IN, Watts KE, Schmitt AK, Morgan LA, Shanks PWC (2007) Voluminous low- $\delta^{18}\text{O}$ magmas in the late Miocene Heise volcanic field, Idaho: Implications for the fate of Yellowstone hotspot calderas. *Geology* 35:1019-1022
- Bolz V (2001) The oxygen isotope geochemistry of zircon as a petrogenetic tracer in high temperature contact metamorphic and granitic rocks. MS Thesis, University of Edinburgh, Scotland.
- Chacko T, Cole DR, Horita J (2001) Equilibrium oxygen, hydrogen and carbon isotope fractionation factors applicable to geologic systems. *Rev Mineral Geochem* 43:1-81
- Charlier BLA, Wilson CJN, Lowenstern JB, Blake S, Van Calsteren PW, Davidson JP (2005) Magma generation at a large hyperactive silicic volcano (Taupo New Zealand) revealed by U-Th and U-Pb systematics in zircons. *J Petrol* 46:3-32
- Chiba H, Chacko T, Clayton RN, Goldsmith JR (1989) Oxygen isotope fractionations involving diopside, forsterite, magnetite, and calcite: Application to geothermometry. *Geochim Cosmochim Acta* 53:2985-2995
- Coleman DS, Gray W, Glazner AF (2004) Rethinking the emplacement and evolution of zoned plutons: Geochronologic evidence for incremental assembly of the Tuolumne Intrusive Suite, California. *Geology* 32:433-436
- Cooper KM, Reid MR (2008) Uranium-series crystal ages. *Rev Mineral Geochem* 69:479-554
- Costa F, Dohmen R, Chakraborty S (2008) Time scales of magmatic processes from modeling the zoning patterns of crystals. *Rev Mineral Geochem* 69:545-594
- Costa F, Dungan M (2005) Short time scales of magmatic assimilation from diffusion modeling of multiple elements in olivine. *Geology* 33:837-840
- Crank J (1975) *The Mathematics of Diffusion*, 2nd Edition. Oxford: Oxford University Press
- Davidson JP, Tepley F III, Palacz Z, Meffan-Main S (2001) Magma recharge, contamination and residence times revealed by in situ laser ablation isotopic analysis of feldspar in volcanic rocks. *Earth Planet Sci Lett* 184:427-442
- Davies GR, Halliday AN (1998) Development of the Long Valley rhyolitic magma system: Sr and Nd isotope evidence from glasses and individual phenocrysts. *Geochim Cosmochim Acta* 62:3561-3574
- de Silva SL, Gosnold WD (2007) Episodic construction of batholiths: insights from the spatiotemporal development of an ignimbrite flare-up. *J Volcanol Geotherm Res* 167:320-335

- Dorendorf F, Wiechert U, Worner G (2000) Hydrated sub-arc mantle: A source for the Klyuchevskoy volcano, Kamchatka/Russia. *Earth Planet Sci Lett* 175:69-86
- Dufek J, Bergantz GW (2005) Lower crustal magma genesis and preservation: A stochastic framework for the evaluation of basalt-crust interaction. *J Petrology* 46: 2167-2195
- Dungan MA, Davidson J (2004) Partial assimilative recycling of the mafic plutonic roots of arc volcanoes: An example from the Chilean Andes. *Geology* 32:773-776
- Eiler JM (2001) Oxygen isotope variations in basaltic lavas and upper mantle rocks. *Rev Mineral Geochem* 43:319-364
- Eiler JM, Valley JW, Baumgartner LP (1993) A new look at stable isotope thermometry. *Geochim Cosmochim Acta* 57:2571-2583
- Elphick SC, Dennis PF, Graham CM (1986) An experimental-study of the diffusion of oxygen in quartz and albite using an overgrowth technique. *Contrib Mineral Petrol* 92:322-330
- Elphick SC, Graham CM, Dennis PF (1988) An ion microprobe study of anhydrous oxygen diffusion in anorthite - a comparison with hydrothermal data and some geological implications. *Contrib Mineral Petrol* 100:490-495
- Farquhar J, Chacko T, Frost BR (1993) Strategies for high-temperature oxygen-isotope thermometry - a worked example from the Laramie anorthosite complex, Wyoming, USA. *Earth Planet Sci Lett* 117:407-422
- Farver JR (1989) Oxygen self-diffusion in diopside with application to cooling rate determinations. *Earth Planet Sci Lett* 92:386-396
- Farver JR, Yund RA (1991) Oxygen diffusion in quartz: dependence on temperature and water fugacity. *Chem Geol* 90:55-70
- Finney B, Turner S, Hawkesworth C, Larsen J, Nye C, George R, Bindeman I, Eichelberger J (2008) Magmatic differentiation at an island-arc caldera: Okmok volcano, Aleutian Islands, Alaska. *J Petrol* doi:10.1093/petrology/egn008
- Friedman I, Lipman PW, Obradovich JD, Gleason JD, Christiansen RL (1974) Meteoric water in magmas. *Science* 184:1069-1072
- Friedman I, O'Neil JR (1977) Compilation of stable isotope fractionation factors of geochemical interest (Geological Survey Professional Paper 440-KK. *In*: Data of Geochemistry, 6th Ed. Fleischer M (ed) Washington, D.C., U.S. Gov Print Off p. 1-12
- Gansecki CA, Mahood GA, McWilliams MO (1996) $^{40}\text{Ar}/^{39}\text{Ar}$ geochronology of rhyolites erupted following collapse of the Yellowstone caldera, Yellowstone Plateau volcanic field: implications for crustal contamination. *Earth Planet Sci Lett* 142:91-107
- Garcia MO, Ito E, Eiler JM (2008) Oxygen isotope evidence for chemical interaction of Kilauea historical magmas with basement rocks. *J Petrol* 49:757-769
- Garcia MO, Ito E, Eiler JM, Pietruszka AJ (1998) Crustal contamination of Kilauea Volcano magmas revealed by oxygen isotope analyses of glass and olivine from Puu Oo eruption lavas. *J Petrol* 39:803-817
- Ghiorso MS, Sack RO (1995) Chemical mass transfer in magmatic processes. 4. A revised and internally consistent thermodynamic model for the interpolation and extrapolation of liquid-solid equilibria in magmatic systems at elevated temperatures and pressures. *Contrib Mineral Petrol* 119:197-212
- Glazner AF, Bartley JM, Coleman DS, Gray W, Taylor RZ (2004) Are plutons assembled over millions of years by amalgamation from small magma chambers? *GSA Today* 14:4-11
- Grunder AL (1995) Material and thermal roles of basalt in crustal magmatism: A case study from eastern Nevada. *Geology* 23:952-956
- Gurenko AA, Chaussidon M (2002) Oxygen isotope variations in primitive tholefites of Iceland: evidence from a SIMS study of glass inclusions, olivine phenocrysts and pillow rim glasses. *Earth Planet Sci Lett* 205:63-79
- Gurenko AA, Sobolev AV (2006) Crust-primitive magma interaction beneath neovolcanic rift zone of Iceland recorded in gabbro xenoliths from Midfell, SW Iceland. *Contrib Mineral Petrol* 151:495-520
- Hanchar JM, Hoskin PWO (eds) (2003) Zircon. *Reviews in Mineralogy and Geochemistry* Vol. 53, Mineralogical Society of America, Washington, D.C.
- Harmon RS, Hoefs J (1995) Oxygen-isotope heterogeneity of the mantle deduced from global O-18 systematics of basalts from different geotectonic settings. *Contrib Mineral Petrol* 120:95-114
- Hildreth W, Christiansen RL, O'Neil JR (1984) Catastrophic isotopic modification of rhyolitic magma at times of caldera subsidence, Yellowstone Plateau Volcanic Field. *J Geophys Res* 89:8339-8369
- Hildreth W, Halliday AN, Christiansen RL (1991) Isotopic and chemical evidence concerning the genesis and contamination of basaltic and rhyolitic magmas beneath the Yellowstone Plateau Volcanic Field. *J Petrol* 32:63-138
- Hinton RW (1995) Ion microprobe analysis in geology. *In*: Microprobe Techniques in the Earth Sciences. PJ Potts, JFW. Bowles, SJB. Reed and MR Cave (eds). London, Chapman and Hall: 235-289
- Hoefs J (2005) *Stable Isotope Geochemistry*, Springer, 5th edition

- Ireland TR (1995) Ion microprobe mass spectrometry: techniques and applications in cosmochemistry, geochemistry, and geochronology. *In: Advances in Analytical Geochemistry*. Hyman M, Rowe MW (eds). London, JAI Press Inc. 2:1-118
- Johnson CM, Beard BL, Albarede F (eds) (2004) *Geochemistry of Non-Traditional Stable Isotopes*. Rev Mineral Geochem, volume 55. Mineralogical Society of America
- Kalamarides RI (1984) Kiglapait geochemistry VI: Oxygen isotopes. *Geochim Cosmochim Acta* 48:1827-1836
- King EM, Valley JW (2001) The source, magmatic contamination, and alteration of the Idaho batholith. *Contrib Mineral Petrol* 142:72-88
- Kita NT, Ikeda Y, Togashi S, Liu YZ, Morishita Y, Weisberg MK (2004) Origin of ureilites inferred from a SIMS oxygen isotopic and trace element study of clasts in the Dar al Gani 319 polymict ureilite. *Geochim Cosmochim Acta* 68: 213-4235
- Krylov DP, Zagnitko VN, Hoernes S, Lugovaja IP, Hoffbauer R (2002) Oxygen isotope fractionations between zircon and water: Experimental determination and comparison with quartz-zircon calibrations. *Eur J Mineral* 14:849-853
- Kyser TK, O'Neil JR, Carmichael ISE (1982) Genetic relations among basic lavas and ultramafic nodules: Evidence from oxygen isotope compositions. *Contrib Mineral Petrol* 81:88-102
- Lackey JS, Valley JW, Hinke HJ (2006) Deciphering the source and contamination history of peraluminous magmas using delta 18-O of accessory minerals: examples from garnet-bearing plutons of the Sierra Nevada batholith. *Contrib Mineral Petrol* 151:20-44
- Lackey JS, Valley JW, Saleeby JB (2005) Supracrustal input to magmas in the deep crust of Sierra Nevada batholith: Evidence from high-delta O-18 zircon. *Earth Planet Sci Lett* 235:315-330
- Lanphere MA, Champion DE, Christiansen RL, Izett GA, Obradovich JD (2002) Revised ages for tuffs of the Yellowstone Plateau volcanic field: Assignment of the Huckleberry Ridge Tuff to a new geomagnetic polarity event. *Geol Soc Am Bull* 114:559-568
- MacPherson GJ, Mittlefehldt DW, Jones JH, Simon SB, Papke JJ, Mackwell S (eds) (2008) *Oxygen in the Solar System*. Rev Mineral Geochem, volume 68. Mineralogical Society of America
- Marsh BD (1998) On the interpretation of crystal size distributions in magmatic systems. *J Petrol* 39:553-599
- Matthews A, Palin JM, Epstein S, Stolper EM (1994) Experimental study of ¹⁸O/¹⁶O partitioning between crystalline albite, albitic glass and CO₂ gas. *Geochim Cosmochim Acta* 58:5255-5266
- Matthews A, Stolper EM, Eiler JM, Epstein S (1998) Oxygen isotope fractionation among melts, minerals and rocks. *In: Proceedings of the 1998 Goldsmith Conference, Toulouse*, pp. 971-972. London Mineralogical Society.
- McBirney AR (2006) *Igneous Petrology*, 3rd Edition, Johns and Bartlett
- Miller JS, Wooden JL (2004) Residence resorption and recycling of zircons in Devils Kitchen rhyolite Coso Volcanic Field, California. *J Petrol* 45:2155-2170
- Mills JG Jr., Saltoun BW, Vogel TA (1997) Magma batches in the Timber Mountain magmatic system SW Nevada volcanic field Nevada, USA. *J Volcanol Geotherm Res* 78:185-208
- Morgan LA, McIntosh WC (2005) Timing and development of the Heise volcanic field, Snake River Plain, Idaho, western USA. *Geol Soc Am Bull* 117:288-306
- Morishita Y, Gilette BJ, Farver JR (1996) Volume self-diffusion of oxygen in titanite: *Geochem J* 30:71-79
- Muehlenbachs K, Anderson AT, Sigvaldasson GE (1974) Low-δ¹⁸O basalts from Iceland. *Geochim Cosmochim Acta* 38:577-588
- Muehlenbachs K (1998) The oxygen isotopic composition of the oceans, sediments and the seafloor. *Chem Geol* 145:263-273
- Obradovich JD (1992) K-Ar ages of Yellowstone Volcanic Field volcanic rocks. *US Geol Surv Open File Rep* 92408
- Page FZ, Ushikubo T, Kita NY, Riciputi LR, Valley JW (2007) High precision oxygen isotope analysis of picogram samples reveals 2-μm gradients and slow diffusion in zircon. *Am Mineral* 92:1772-1775
- Palin JM, Stolper EM, Epstein S (1996) Oxygen isotope partitioning between rhyolitic glass/melt and CO₂: an experimental study at 550-950 degrees C and 1 bar. *Geochim Cosmochim Acta* 60:1963-1973
- Portnyagin M, Bindeman IN, Hoernle K, Hauff F (2007) *Geochemistry of primitive lavas of the Central Kamchatka Depression*. *In: Magma Generation at the Edge of the Pacific Plate*. AGU Monograph series 172 "Volcanism and Subduction: the Kamchatka Region" p. 199-239
- Ramos FC, Tepley FJ III (2008) Inter- and intracrystalline isotopic disequilibria: techniques and applications. *Rev Mineral Geochem* 69:403-443
- Reid MR (2003) Timescales of magma transfer and storage in the crust. *In: The Crust, Treatise on Geochemistry*, Vol. 3. Rudnick RL (ed) Elsevier, Oxford, UK. p 167-193
- Reid MR Coath CD (2000) In situ U-Pb ages of zircons from the Bishop Tuff: No evidence for long crystal residence times. *Geology* 28:443-446

- Riciputi LR, Paterson BA, Ripperdan RL (1998) Measurement of light stable isotope ratios by SIMS: Matrix effects for oxygen, carbon, and sulfur isotopes in minerals. *Int J Mass Spectrom* 178:81-112
- Rumble D, Farquhar J, Young ED, Christensen CP (1997) In situ oxygen isotope analysis with an excimer laser using F2 and BrF5 reagents and O-2 gas as analyte. *Geochim Cosmochim Acta*: 61:4229-4234
- Ryerson FJ, Durham WD, Cherniak DJ (1989) Oxygen diffusion in olivine- effect of oxygen fugacity and implications for creep. *J Geophys Res Solid Earth* 94:4105-4118
- Schmitt AK, Grove M, Harrison TM, Lovera O, Hulen JB, Walters M (2003a) The Geysers - Cobb Mountain Magma System California (Part 1): U-Pb zircon ages of volcanic rocks conditions of zircon crystallization and magma residence times. *Geochim Cosmochim Acta* 67:3423-3442
- Schmitt AK, Grove M, Harrison TM, Lovera O, Hulen JB, Walters M (2003b) The Geysers-Cobb Mountain Magma System California (Part 2): Timescales of pluton emplacement and implications for its thermal history. *Geochim Cosmochim Acta* 67:3443-3458
- Sharp Z (2006) Principles of Stable isotope Geochemistry. Prentice Hall
- Sharp ZD (1990) A laser-based microanalytical method for the in situ determination of oxygen isotope ratios of silicates and oxides. *Geochim Cosmochim Acta* 54:1353-1357
- Sigmarrsson O, Condomines M, Gronvold K, Thordarson T (1991) Extreme magma homogeneity in the 1783-84 Lakagigar eruption: origin of a large volume of evolved basalt in Iceland. *Geophys Res Lett* 18:2229-2232
- Simakin AG, Bindeman IN (2008) Evolution of crystal sizes in the series of dissolution and precipitation events in open magma systems. *J Volcanol Geotherm Res* doi: 10.1016/j.jvolgeores.2008.07.012
- Simon JJ, Reid MR (2005) The pace of rhyolite differentiation and storage in an 'archetypical' silicic magma system Long Valley. *Earth Planet Sci Lett* 235:123-140
- Spera FJ, Bohron WA (2004) Open-system magma chamber evolution: an energy-constrained geochemical model incorporating the effects of concurrent eruption, recharge, variable assimilation and fractional crystallization. *J Petrol* 45:2459-2480
- Streck MJ (2008) Mineral textures and zoning as evidence for open system processes. *Rev Mineral Geochem* 69:595-622
- Taylor HP (1968) The oxygen isotope geochemistry of igneous rocks. *Contrib Mineral Petrol* 19:1-71
- Taylor HP Jr. (1980) The effects of assimilation of country rocks by magmas on O¹⁸-O¹⁶ and Sr⁸⁷/Sr⁸⁶ systematics in igneous rocks. *Earth Planet Sci Lett* 47:243-254
- Taylor HP Jr. (1986) Igneous rocks: II. Isotopic case studies of circum-pacific magmatism. *Rev Mineral* 16:273-316
- Taylor HP Jr., Sheppard SMF (1986) Igneous rocks: I. Processes of isotopic fractionation and isotopic systematics. *Rev Mineral* 16:227-272
- Tefend KS, Vogel TA, Flood TP, Ehrlich R (2007) Identifying relationships among silicic magma batches by polytopic vector analysis: A study of the Topopah Spring and Pah Canyon Ash-flow Sheets of the Southwest Nevada Volcanic Field. *J Volcanol Geotherm Res* 167:198-211
- Tepley FJ, Davidson JP (2003) Mineral-scale Sr-isotope constraints on magma evolution and chamber dynamics in the Rum layered intrusion, Scotland. *Contrib Mineral Petrol* 145:628-641
- Tepley FJ, Davidson JP, Clyne MA (1999) Magmatic interactions as recorded in plagioclase phenocrysts of Chaos Crags, Lassen Volcanic Center, California. *J Petrol* 40:787-806
- Thordarson T, Self S (2003) Atmospheric and environmental effects of the 1783-1784 Laki eruption: A review and reassessment. *J Geophys Res.-Atm D1 Article Number*: 4011
- Trail D, Bindeman IN, Watson EB (2008) Experimental determination of quartz-zircon oxygen isotope fractionation. (in prep)
- Urey HC (1947) The thermodynamic properties of isotopic substances. *J Chem Soc (Lond)* 1947:562-581
- Valley JW (2001) Stable isotope thermometry at high temperatures. *Rev Mineral Geochem* 43:365-413
- Valley JW (2003) Oxygen isotopes in zircon. *Rev Mineral Geochem* 53:343-385
- Valley JW, Bindeman IN, Peck WH (2003) Calibration of zircon-quartz oxygen isotope fractionation. *Geochim Cosmochim Acta* 67:3257-3266
- Valley JW, Cole D (eds) (2001) Stable Isotope Chemistry. *Rev Geochem Mineral*, volume 43. Mineralogical Society of America
- Valley JW, Kinny PD, Schulze DJ, Spicuzza MJ (1998) Zircon megacrysts from kimberlite: oxygen isotope variability among mantle melts. *Contrib Mineral Petrol* 133:1-11
- Valley JW, Kitchen N, Kohn MJ, Niendorf CR, Spicuzza MJ (1995) UWG-2, a garnet standard for oxygen isotope ratio: strategies for high precision and accuracy with laser heating. *Geochim Cosmochim Acta*. 59:5223-5231
- Valley JW, Lackey JS, Cavosie AJ, Clechenko C, Spicuzza MJ, Basei MAS, Bindeman IN, Ferreira VP, Sial AN, King EM, Peck WH, Sinha AK, Wei CS (2005) 4.4 billion years of crustal maturation: oxygen isotope ratios of magmatic zircon. *Contrib Mineral Petrol* 150:561-580

- Valley JW, Taylor HP Jr., O'Neil JR (eds) (1986) Stable Isotopes in High Temperature Geological Processes. Rev Geochem Mineral, volume 16. Mineralogical Society of America
- Vazquez JA, Reid MR (2002). Time scales of magma storage and differentiation of voluminous high-silica rhyolites at Yellowstone caldera, Wyoming. *Contrib Mineral Petrol* 144:274-285
- Wallace PJ, Anderson AT, Davis AM (1999) Gradients in H₂O, CO₂, and exsolved gas in a large-volume silicic magma system: Interpreting the record preserved in melt inclusions from the Bishop Tuff. *J Geophys Res* 104:20097-20122
- Wang ZG, Kitchen NE, Eiler JM (2003) Oxygen isotope geochemistry of the second HSDP core. *Geochim Geophys Geosystems* 4 Article Number: 8712
- Wark DA, Spear FS, Cherniak DJ, Watson EB (2007) Pre-eruption recharge of the Bishop magma system. *Geology* 35:235-238
- Wark DA, Watson EB (2006) TitaniQ: A titanium-in-quartz geothermometer. *Contrib Mineral Petrol* 152:743-754
- Watson EB (1996) Dissolution, growth and survival of zircons during crustal fusion: Kinetic principles, geological models and implications for isotopic inheritance. *Trans R Soc Edinburgh: Earth Sci* 87:43-56
- Watson EB, Cherniak DJ (1997) Oxygen diffusion in zircon. *Earth Planet Sci Lett* 148:527-544
- Williams DA, Kadel SD, Greeley R, Leshner CM, Clyne MA (2004) Erosion by flowing lava: geochemical evidence in the Cave Basalt, Mount St. Helens, Washington. *Bull Volcanol* 66:168-181
- Williams DA, Kerr RC, Leshner CM, Barnes SJ (2001) Analytical/numerical modeling of komatiite lava emplacement and thermal erosion at Perseverance, Western Australia. *J Volcanol Geotherm Res* 110:27-55.
- Wolff JA, Ramos FC (2003) Pb isotope variations among Bandelier Tuff feldspars: no evidence for a long-lived silicic magma chamber. *Geology* 31:533-536
- Young ED, Fogel ML, Rumble D, Hoering TC (1998) Isotope-ratio-monitoring of O₂ for microanalysis of O¹⁸/O¹⁶ and O¹⁷/O¹⁶ in geological materials. *Geochim Cosmochim Acta* 62:3087-3094
- Young ED, Kuramoto K, Marcus RA, Yurimoto H, Jacobsen SB (2008) Mass-independent oxygen isotope variation in the solar nebula. *Oxygen in the solar system: Rev Mineral Geochem* 68:187-218
- Zhang YX, Walker D, Leshner CE (1989) Diffusive crystal dissolution. *Contrib Mineral Petrol* 102:492-513
- Zhao Z, Zheng Y-F (2003) Calculation of oxygen isotope fractionation in magmatic rocks. *Chem Geol* 193:59-80
- Zheng YF (1993a) Calculation of oxygen isotope fractionation in anhydrous silicate minerals. *Geochim Cosmochim Acta* 57:1079-1091
- Zheng YF (1993b) Calculation of oxygen-isotope fractionation in hydroxyl-bearing silicates. *Earth Planet Sci Lett* 120:247-263